A GRAVITY SURVEY ACROSS THE MT LOFTY RANGES

SOUTH AUSTRALIA

M. P. Middleton, B.Sc.

A thesis submitted as part of the
requirements of the Honours Degree
of Bachelor of Science (Geophysics)

Adelaide

October   1973

Supervisors: D M Boyd, P I Brooker

Acknowledgements

For supervision throughout the year leading to the preparation of
this thesis, I express my gratitude to Professor D. M. Boyd and
Dr. P. I. Brooker, of the University of Adelaide.

For helpful criticism and suggestions, I am also grateful to my
Honours and Research colleagues.

Field work would not have been possible without the assistance of
Geosurveys of Australia Pty. Limited, and the Engineering and Water
Supply Department. In particular, I wish to thank Messrs. R.C. Sprigg,
D.H.A. von Sanden, P.G. Brunt and J. Radus.

M. P. Middleton

October, 1973

ABSTRACT

A gravity survey across the central Mt. Lofty Ranges produced a
detailed profile linking the Adelaide Plains with the Murray Basin.
The profile is incorporated in a new Bouguer Anomaly Map for the
Adelaide-Mannum area.

Indirect density measurements were obtained from the gravity data,
and these were used in establishing a table of surface-rock densities
for major units encountered in the survey.

Analyses of the regional gravity picture tend to suggest that the
crust thickens asymmetrically eastward under the Ranges.

Computer modelling revealed the probable attitudes of the Palmer and
Eden Faults, the western Archaean/Proterozoic boundary, and also the
position and attitude of the eastern truncation of the Palmer
Granites.

CONTENTS

FIGURES AND PLATES

S.A.

LOCALITY MAP

0 100 200 300
km

1:8000000
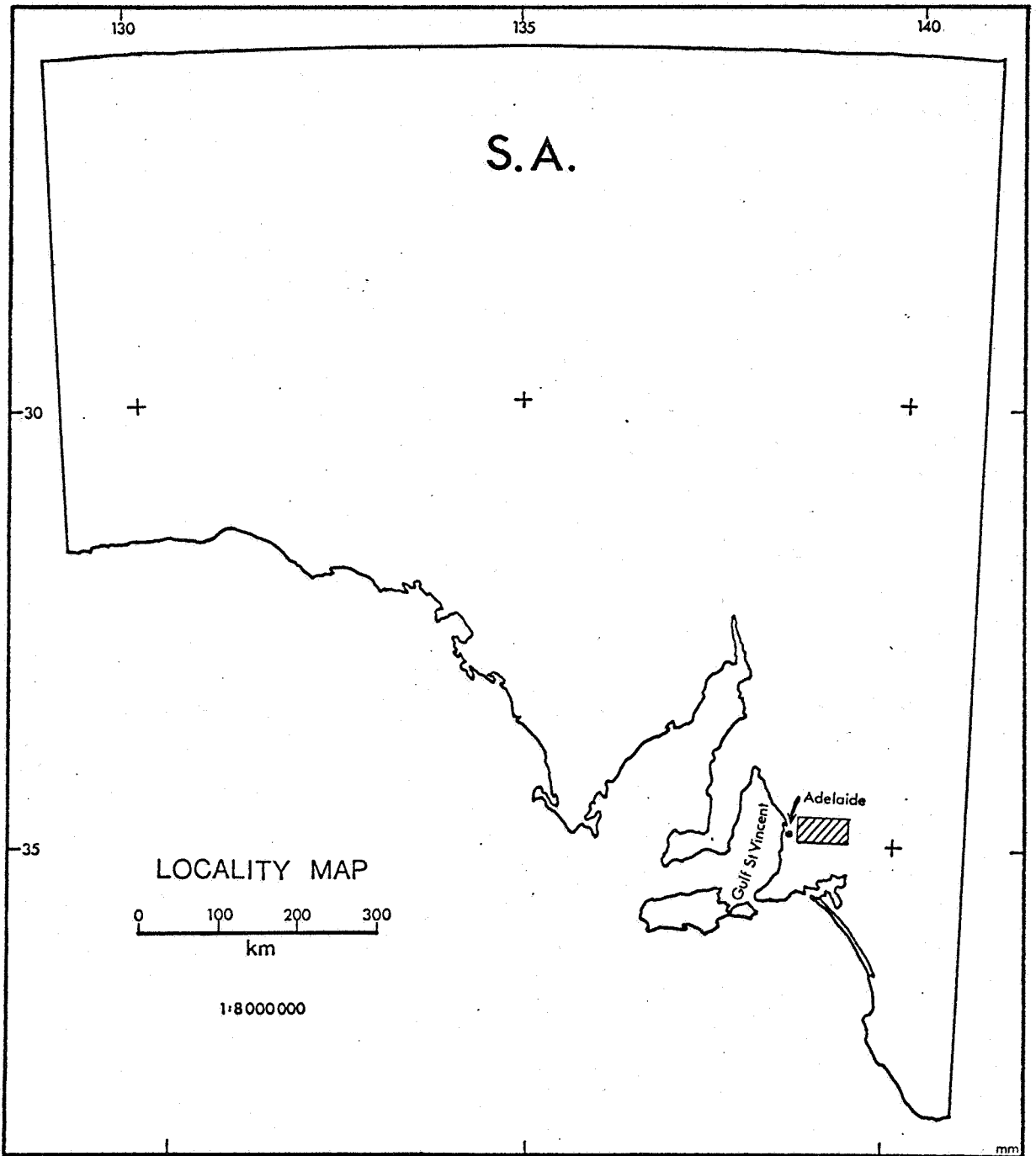
Gulf St Vincent

Adelaide

FIGURE 1

Introduction

The accurately determined elevations along the length of the Mannum-Adelaide Pipeline provide an unusual but convenient traverse along which a gravity survey was conducted.

A traverse such as this offers unusual accessibility to somewhat rugged topography, and has the advantages of being precisely surveyed and of providing stations with a degree of permanence and continuity.

The profile follows a slightly bowed path across the central Mt. Lofty Ranges near the 34° 50'S line of latitude, and is shown on the Bouguer Anomaly overlay of Figure 2 (the line X-Y joins every fifth gravity station). The survey is particularly well suited to follow-up work. Base stations are easily located, and are never far from main roads. Since the western end of the traverse ends near Grand Junction Road, the profile can be extended colinearly a further 18 km to the edge of the Gulf of St. Vincent.

Field work, which was essentially a one-man operation, extended from late June until early August, 1973. The data obtained (measured to the accuracy of commercial surveys) provided a total of 313 gravity stations at an average spacing of just under 200 metres. Terrain corrections, which required some 200 hours of field work and manual computation, were applied to all stations.

Previous surveys across the Ranges have been of a regional nature, and this profile is, perhaps, the first detailed gravity examination across the Ranges. The raw data has been carefully reduced and is included in Appendix D to enable any part of the reduction or subsequent analysis to be reproduced. The results have been incorporated in the Bouguer Anomaly Map of Figure 2.

The analysis of the survey data is the main subject of this thesis. The reduced data is first examined to obtain indirect density measurements which are used in compiling a table of surface-rock densities for units encountered in the survey. Knowledge of these densities allows individual anomalies to be more accurately defined, and also aids in assigning realistic density contrasts to geophysical models.

A regional-residual separation is carried out, and the resulting regional and residual anomalies are analysed. Quantitative interpretation is based largely on computer modelling, and known geology forms the primary control. Many problems were encountered in time delays associated with processing, but some measure of success was achieved in obtaining satisfactory models, and these will be described in later sections.

Wherever possible, routine or ancillary data and calculations have been relegated to appendices.

I. Survey Procedure

Some of the advantages peculiar to a survey along a major pipeline have already been mentioned. Another useful feature is that any point along the 60-km length of the Mannum-Adelaide Pipeline can be uniquely defined by a single co-ordinate. The co-ordinate fixes the position of a point whether it is to be referred to a map, a profile, or a physical position along the pipeline. This co-ordinate is called the "chainage" or, simply, the "distance", and, in this thesis, it begins at an arbitrary origin and increases eastward. The absolute value of the chainage with respect to the pipeline itself is explained in Appendix D.

The chainage, of course, is calculated as a true distance along the axis of the pipeline itself. It should be borne in mind that the pipeline is neither straight nor horizontal. For the purposes of this analysis, however, there is no significant distortion with respect to the horizontal, and, except over large distances, the pipeline is reasonably straight.

Since the pipeline possesses a mass, its significance must be determined. This is, however, complicated by the fact that the mass varies according to the water content of the pipe. This point is discussed in Appendix A, but it may be noted here that the gravitational effect of the pipeline may be neglected a short distance away from it.

The assigning of an accurate elevation to each gravity station is an integral part of any gravity survey, but it posed an unusual problem in this survey.

Favourable points were first chosen from "as constructed" Plans, and their chainages noted. Each point had to be pinpointed on the pipeline by carefully measuring from at least two nearby distinctive objects whose chainages were also known. The accuracy of this procedure is discussed in Appendix B, but it may be remarked here that many old survey-markers were located by this method. When the point was located, a station was marked. Subsequently, measurements from the underside of the pipe were made to a suitable point on the ground to determine the ground elevation. (Although elevations to the ground were also given on the plans, it was found that, in many instances, ground levels had appreciably shifted since construction of the pipeline in the 1940s).

This procedure proved to be very time consuming, and stations were covered at a rate of only 25 per day.

In many instances there was little choice for the position of a station, and often it was impossible to avoid placing stations on hillsides or in cuttings. In normal surveys it is often possible to avoid such positions. Accordingly, many stations required relatively high inner-zone terrain corrections.

Initial problems were experienced with a La Coste & Romberg gravimeter when drift rates up to 0.20 mgal/h were observed, and significant discrepancies occurred on re-readings. A second meter (also a La Coste & Romberg) was used to re-run all base networks and initial stations, and excellent drift characteristics were noted with this.

Tidal corrections, which were calculated to vary at rates of up to 0.05 mgal/h with daily amplitudes of up to 0.19 mgal, were applied to all readings. Residual drift was usually less than 0.03 mgal over an average $3\frac{1}{2}$-h period.

Up to 55 stations per day were read with the gravimeter. The quoted instrument factor, though normally adopted for this type of meter, was found to be unsatisfactory when compared with several runs over the Adelaide Calibration Range, and the measured factor was adopted.

Microseisms were noted on 3 occasions, while vibration from wind and pumping forced meter reading to be abandoned on a further 3 occasions.

Terrain Corrections

Prior to evaluation of latitude and terrain corrections, all stations were plotted onto a series of plans and maps ranging in scale from 1:4800 to 1:250 000.

Terrain corrections were evaluated according to the techniques described by Hammer (1939) and Sandberg (1958).

The high station-density allowed some flexibility in evaluating the corrections. Measurements showed that zones G, H and I (outer radii 1.5, 2.6, 4.4 km) varied quite slowly and, in most cases, could be evaluated every sixth or eighth station and the remainder interpolated. Zone F (o.r. 0.9 km) was evaluated every 3rd station if station elevations were similar, while Zone E (o.r. 400 m) was scaled individually from a variety of topographic maps. Zones B, C and D were calculated from individual estimates in the field, where 1:4800 plans and the pipeline itself provided convenient yardsticks.

Corrections were taken to Zone I. At a density of 2.67 g/cm^3 corrections varied from 0.02 mgal near Mannum to 1.30 mgal on the western edge of the Ranges, and ironed out many small bumps in the profile. However, the overall shape of the profile altered very little, probably because of the station spacing and overall continuity of the stations.
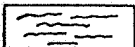
The accuracy of the final measurements is 0.1 mgal (Appendix B).

FIGURE 2

Regional Geological and Bouguer Anomaly maps (1: 250 000)
of the Adelaide - Mannum Area

Bouguer Density: 2.40 g/cm^3

KEY TO GEOLOGY

Quaternary. Mainly Pleistocene sandy clays.

Proterozoic (Adelaide System). Mainly Burra Group.

Tertiary. Lateritic in part.

Stonyfell Quartzite.

Palmer Granite (Cambrian-Ordivician)

Archaean (Barossa Complex)

Rathjen Gneiss (Cambrian-Ordivician)

—— Fault

Kanmantoo Group (Cambrian)

—— — Fault (inferred)

Geology adapted from ADELAIDE 1:250000 and 1:63360 sheets and MANNUM 1:63360 sheet.

Elizabeth

Birdwood

Mannum
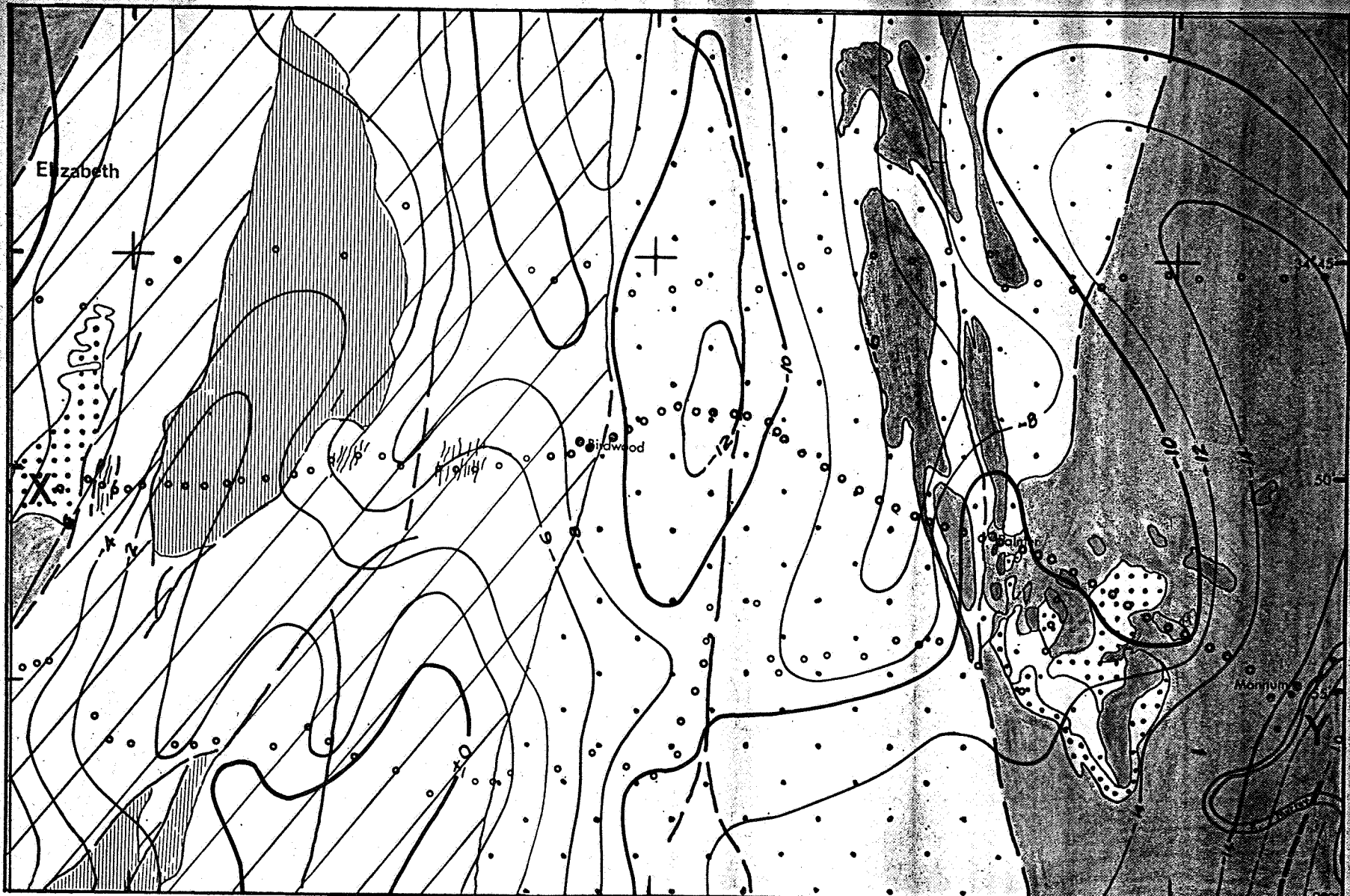
0   45'   5   10

• Gravity Station

km

139°00'

15'

1:250 000

MABOUGER REGIONAL ANOMALY GRAVITY

Contour Interval   2 mgal
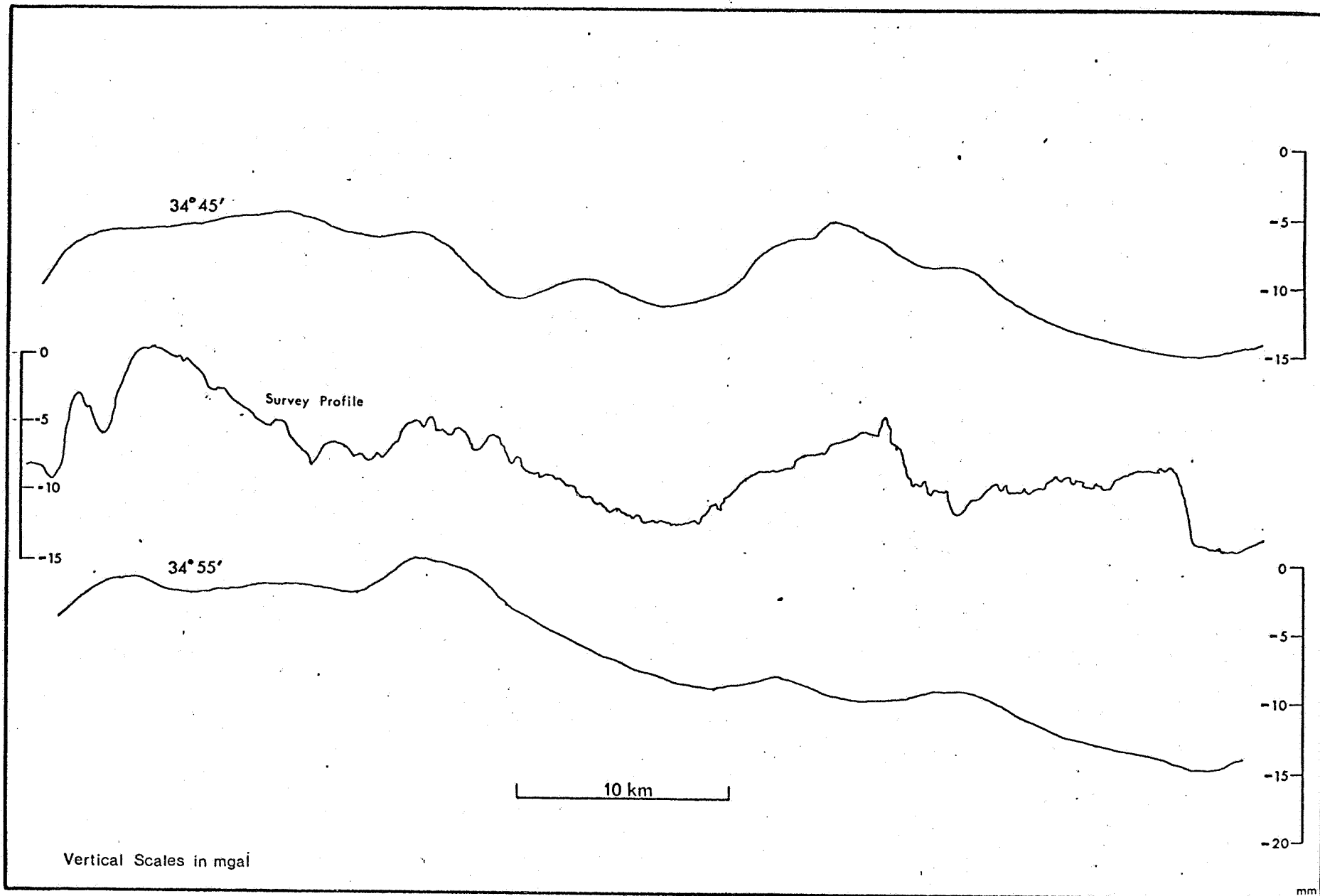
FIGURE 3   Comparison of 3 Regionals
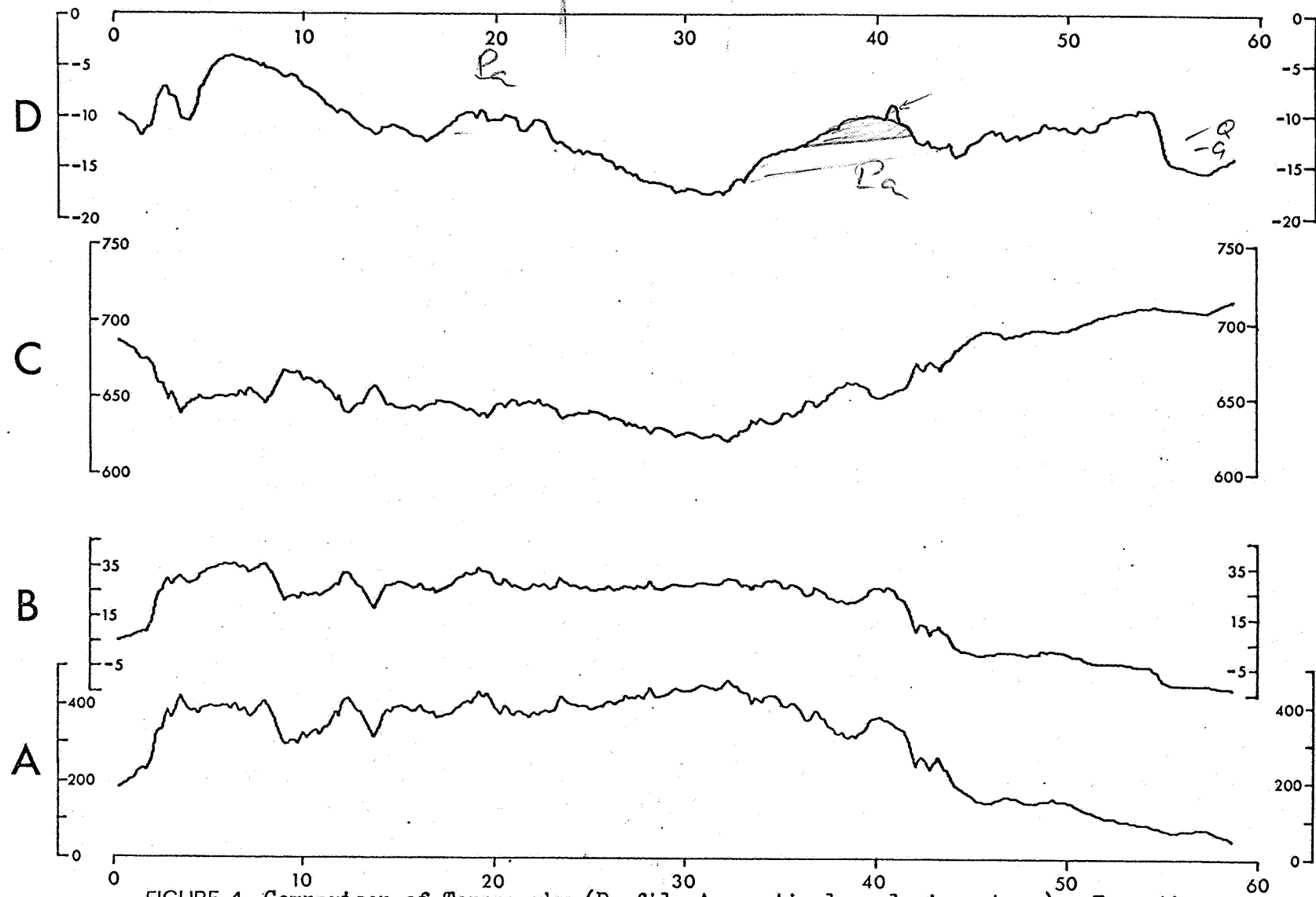
FIGURE 4 Comparison of Topography (Profile A, vertical scale in metres), Free Air Anomaly (B, mgal), Observed Gravity (C, mgal +979000), and Bouguer Anomaly at 2.67 g/cm³ (D, mgal). Horizontal scales in kilometres.

II. Preliminaries

The observed data was comprehensively reduced by standard reduction chains, and the Bouguer Anomaly calculated according to the strict formula

Bouguer Anomaly = Observed Gravity + Free Air Correction –
 Bouguer Slab Correction
 + Terrain Correction – Theoretical Gravity
 at the same latitude

where the theoretical gravity is calculated according to the 1930 International Gravity Formula.

Figure 2 shows the traverse completed in this survey (every fifth station marked). Adjacent gravity stations shown are from regional surveys by Geosurveys of Australia Pty. Ltd. These stations incorporate similar terrain corrections and have been evaluated at a density of 2.4 g/cm^3.

The contour map of Figure 2 has been compiled at this density by incorporating the Geosurveys data with that from this survey, and co-ordinating information from existing maps. The choice of density is examined more fully in the next Section.

For comparison, two regional profiles have been constructed from the contour map, at latitudes 34°45'S and 34°55'S, and these are shown with the survey profile in Figure 3.

The Northern Profile (34°45'S) crosses much the same type of geology as the survey profile, and is very similar in shape and size. Anomaly values are high over the Archaean, more evenly so in the Northern profile, and a central low exists over the middle of the Ranges. This low is flanked by roughly symmetrical kinks or shoulders in both profiles, but the eastern portions are somewhat different. In the Northern profile the values fall off evenly towards the east as Murray Basin sediments gradually thicken from the edge of the outcropping Kanmantoo Group. In the survey profile, however, values drop only slightly at the edge of the Ranges and remain steady before dropping suddenly east of some outcropping granites. Apparently only a thin veil of sediments covers granites before this sudden drop.

The Southern profile (34°55'S) possesses high values in the west over Proterozoic rocks, and differs markedly from the other two profiles in its eastern portion. Values over Kanmantoo rocks are lower and fall off towards the east. As seen by the distortion of the contours over outcropping granites, values are slightly "held up" over the outcrops, and fall off again at their edge. The boundary between granites and Quaternary sediments must be close to the edge of the outcrops here, and veer off towards the north-east (its gravimetric expression fading as it does so).

The survey profile retains major elements of both the North and South profiles. It shows an asymmetrical eastward drop, a central low flanked by two shoulders, high values over Archaean rock, and an interesting anomaly east of outcropping granites.

Figure 4 shows a comparison of Topography, Free Air Anomaly, Observed Gravity, and Bouguer Anomaly at 2.67 g/cm^3. As would be expected, the Free Air Anomaly is closely related to Topography, although it is somewhat flatter in its central portions. If a larger area were involved, this might indicate some degree of non-compensation of an isostatical model, but this would be a bold assertion. The observed gravity, of course, is a reflection of the topography. If these correlations were not observed, the data would be suspect.

The Bouguer Anomaly is relatively flat, and needs to be greatly exaggerated in the vertical direction before comparison with the other profiles. It is evident from this comparison that the Anomaly bears a slight negative correlation with the topography - a feature observed over mountain ranges the world over.

III. Density Determinations

Strictly speaking, any value may be chosen for the density used in reduction to the Bouguer Anomaly. However, it is clearly desirable to eliminate the effect of surface features, as far as possible, by using a realistic measure of the true (average) value of their density. (Density is incorporated in the Bouguer slab approximation and in the terrain correction).

Plate I shows Bouguer Anomaly profiles calculated at five different densities, and their relation to topography. The overall shape of these profiles remains similar regardless of density choice. Absolute values of the anomalies, of course, do change, but we are usually only interested in relative values. On a regional scale, the shape of a profile or a contour map is not particularly sensitive to the density choice, unless there is large relief. This fact was utilised in Figure 2 where a density of 2.4 g/cm^3 was chosen for reduction; here, the primary consideration was to ensure continuity with other available data.

On a local scale, however, density choice can dramatically alter an anomaly's shape, create an apparent anomaly, or destroy a genuine one. For example, referring to Plate I, an anomaly occurs at distance 13.5km over a topographic low. At a density of 2.2 g/cm^3 the anomaly is almost a replica of the topography, but at 2.8 g/cm^3 the anomaly vanishes. For the purpose of interpretation it is clearly desirable to minimise the influence of topographical features by a proper choice of density.

This is the principle of Nettleton's Density Profile method (Nettleton, 1939). A series of profiles, at various densities, are calculated over a topographic feature, and the "density profile" showing the minimum correlation with the feature is selected as the correct density. The method fails if a true subsurface anomaly is being expressed.

The "Bouguer Density" is defined as the density which produces the profile of minimum topographic correlation, and it is taken to be the most appropriate density for use in the Bouguer Anomaly formula. It refers to the density of the surface rocks above a datum (usually) taken as parallel to a smooth surface of regional elevation and passing through topographic minima.

No sampling technique could ever hope to measure (directly) an average density of such a mass of rock, and, in many ways, indirect measurements (that is, those which use the gravity data itself) are superior to direct density measurements (actually taken on rock samples).

Plate I shows that, for any choice of density, small correlations (both positive and negative) exist with topography. This suggests that many topographic features are associated with genuine density contrasts. In seeking to minimise the overall correlation, the Bouguer Density neglects the true structure of the density field, and it should be remembered that this forms a fundamental distinction between "Bouguer" and true density. However, the Bouguer density effectively samples a large mass of rock and yields values consistent with numerous field measurements.

Profiles incorporating variable Bouguer densities are possible, but exceedingly difficult to compile. Vajk (1956) points out that variable densities can only be applied to rocks above the datum previously referred to, while below this datum and down to sea-level, a constant density must be used. It is therefore the usual practice to use one density for any unit under study.

Indirect density measurements require high station-density and appreciable variation in relief. These features are lacking in most surveys, but the present survey is appropriate for studies of this sort, particularly in view of the fact that far too great an area is involved to attempt direct measurements.

Knowledge of appropriate densities for various units (and combinations of units) assists in producing the profiles best suited for interpretation. In addition, it allows realistic density contrasts to be estimated for use in geophysical models.

REGIONAL EFFECTS

It was pointed out (Figure 4) that an overall negative correlation of Bouguer Anomaly with topography exists over the Ranges. This correlation is between regional trends, and tends to mask the localised correlations dealt with in the Density Profile method.

The reader is referred to papers by Vajk (1956) and Grant and Elsaharty (1962) who point out that the literature has failed to emphasize the importance of regional effects in indirect density

determinations. Although regional effects only become important in areas of appreciable relief, it is usually only in such areas that indirect methods can be successfully employed.

When the Density Profile method is used visually, it is reasonably easy for the eye to neglect background regional gradients. In the analyses employed here, however, the method is treated statistically by calculating correlation coefficients at various densities. This requires that the method be expressed in its rare, but correct, form: residual anomalies calculated over residual topography. In other words, broad regional trends must be removed from both the Bouguer Anomaly profiles and also from the topography. (Regional separation is discussed in Section IV).

Plate III shows residual anomalies, at five different densities, compared with residual topography.

Parasnis (1962, p.40) proposes another method of indirect density measurement. Although not stated as such, the method involves taking each station and plotting the Free Air Anomaly against the sum of the Bouguer Slab and Terrain Corrections (both evaluated at unit density). The slope of the resulting straight line (determined by least squares) is taken as the Bouguer Density.

Although Parasnis does not mention it, the elevation used in the Bouguer Slab correction is the residual elevation and not simply the station elevation; residual elevation should also be used in evaluating the Free Air Anomaly (for programming convenience, the equivalent procedure of removing a regional free air anomaly was adopted here). The method is equivalent to assuming that Bouguer Anomalies are random errors. If large anomalies are involved, or there is a preponderance of highs or lows, the method breaks down.

The density determinations described herein are based on the two indirect methods described above. For each unit considered, various combinations of stations were treated. Sometimes large anomalies required exclusion before the methods appeared to work satisfactorily, and in other cases results were not affected. It is clear that the methods require a judicial approach before trends can be accurately defined. For example, studies over Archaean rocks gave, at first, a diversity of solutions. Eventually it became evident that this was because the densities of Archaean rocks appear to increase westward.

Tucker and Brown (1973) summarise density data available from the Flinders Ranges to date. Combined with information from tables and other sources (including inspection of profiles and Figure 2) a framework was formulated on which to base indirect measurements. It was eventually possible to adopt a reasonably narrow range of densities for each major rock unit, while retaining consistency between indirect solutions and all the available information. Table I summarises the adopted densities.

Although regional removal is a key process, studies over the extreme western and eastern stations of the traverse highlighted the difficulties associated with "end-effects" of regional separation. This problem is made more difficult in the present case because the anomaly profile shows relatively high gradients at its extremities. Studies over the Quaternary, and over the profile taken as a whole, were affected by these end-effects.

Figure 5 shows the plot of Free Air Anomaly (mgal)(denoted by Y) against the unit density sum of the Bouguer Slab and Terrain corrections (mgal.g^{-1}.$cm3$) (denoted by X) for the entire profile. The number of stations (n) is 313. The Bouguer density, determined by the least-squares line of best fit (P_s) is 2.63 g/cm^3. Correlation coefficients (ß) at various densities (p) are also shown. If these are plotted against each other, a Bouguer density of 2.63 g/cm3 is also indicated.

Although regionals have not been removed in Figure 5, the two indirect methods give identical answers and indicate a "reasonable" density. Similar studies over the whole profile, but excluding the two extremities, showed that regional separation had very little effect. It is suggested that this is because the regional effects, over this area, tend to balance out.

Over the Quaternary, which occurs on relatively flat terrain, flat regionals would be expected, and it is not surprising that similar observations were made here.

Figure 6, however, shows the dramatic effect of regional removal for other parts of the traverse. Graph (a) shows indirect solutions obtained prior to regional separation, for rocks of the Kanmantoo Group. The least-squares slope method indicates a doubtful density of 1.3 and shows no correspondence with the correlation coefficients. Graph (b), on the other hand, was calculated after regionals had been removed from Bouguer Anomalies and station elevations (and, in this study, from free air anomalies). The solutions look more realistic, and there is close

P	ß
2.2	0.57
2.4	0.35
2.6	0.04
2.8	−0.27
3.0	−0.52

$P_3 = 2.63$

$n = 313$
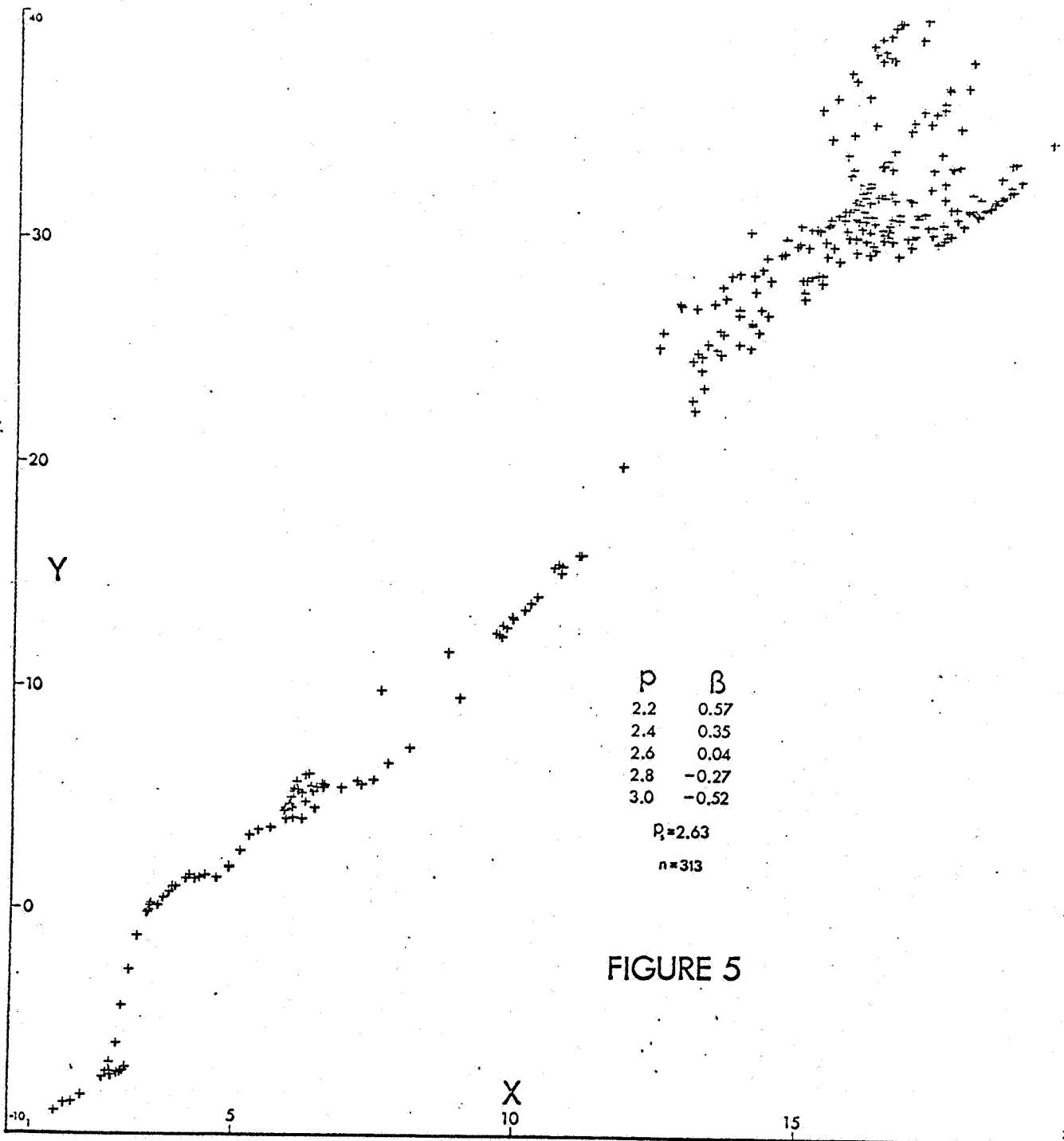
FIGURE 5

Indirect density determinations for the traverse taken as a whole.
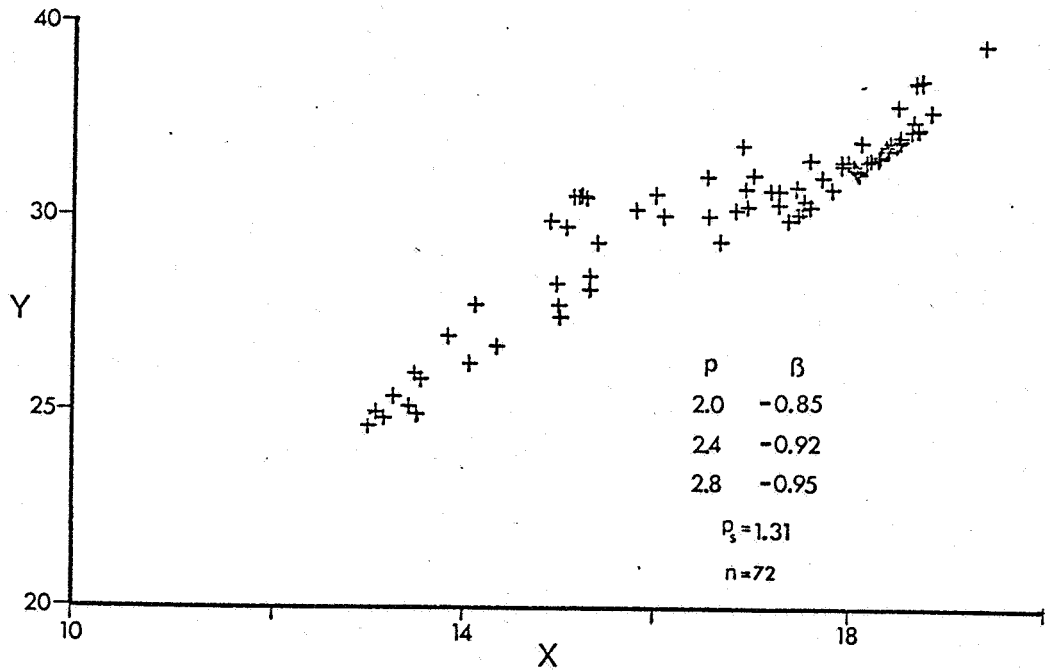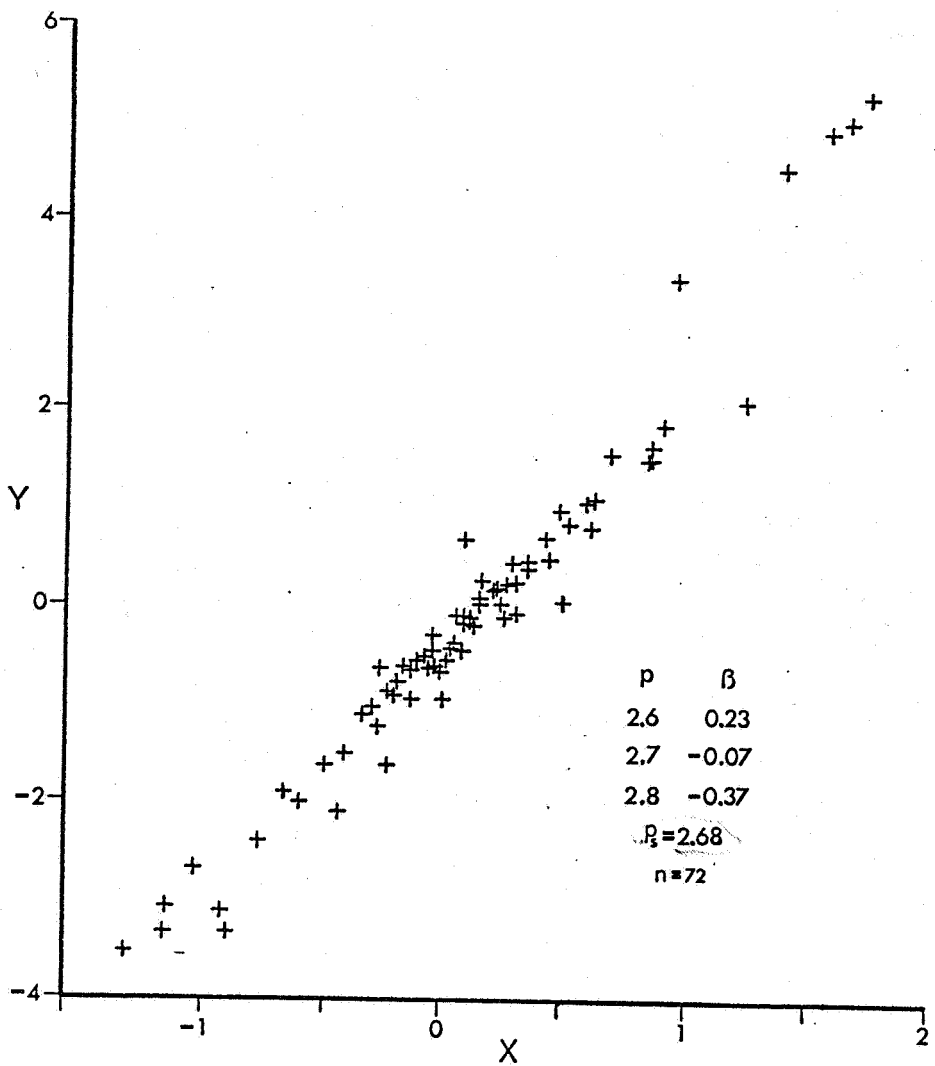
FIGURE 6

Indirect density determinations for the Kanmantoo Group,
(a) before removal of regionals, (b) after removal.

p	ß
2.6	0.27
2.8	−0.04
3.0	−0.29

$p_s = 2.68$

n=97
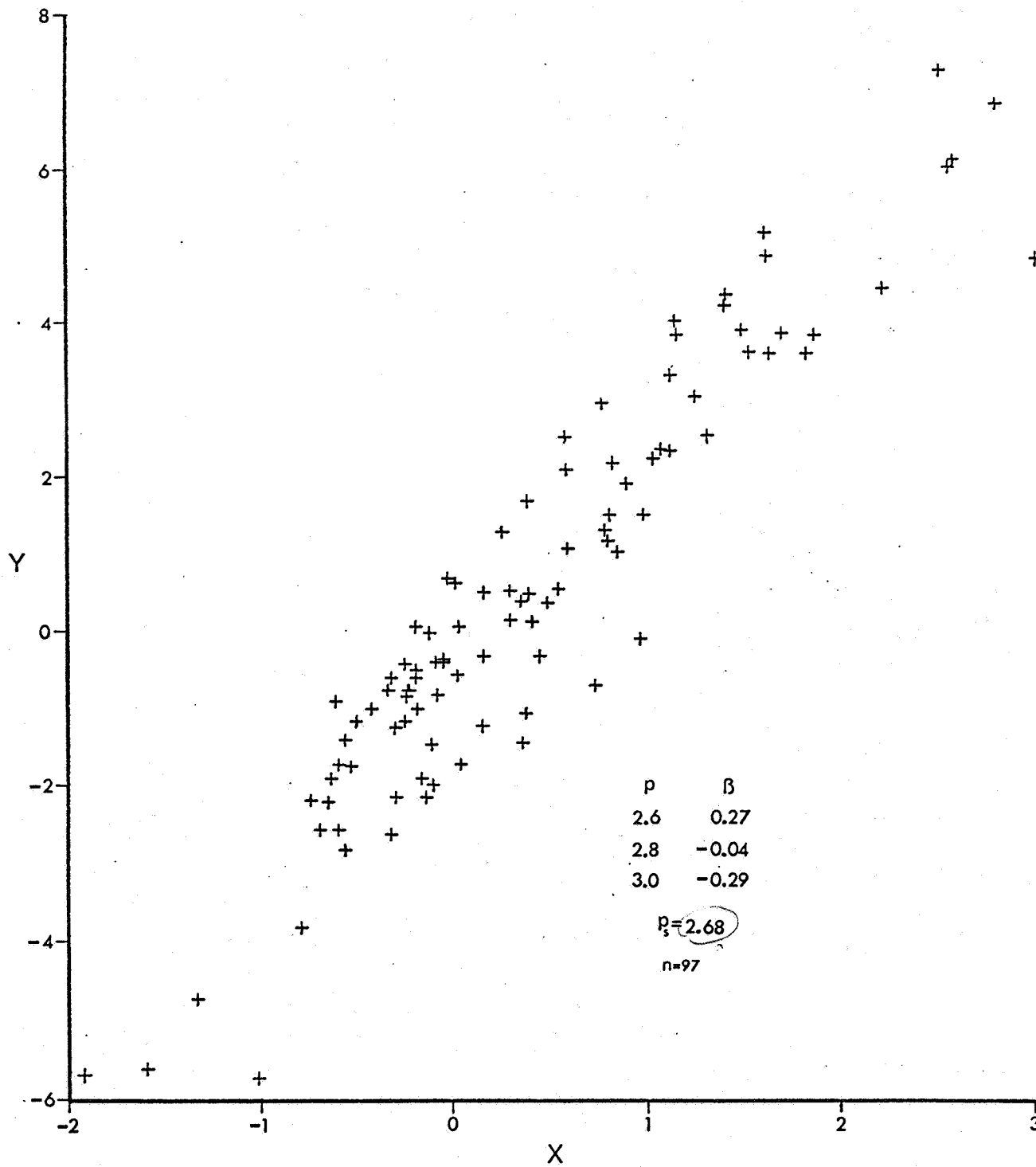
FIGURE 7

Indirect density determinations for the Proterozoic.
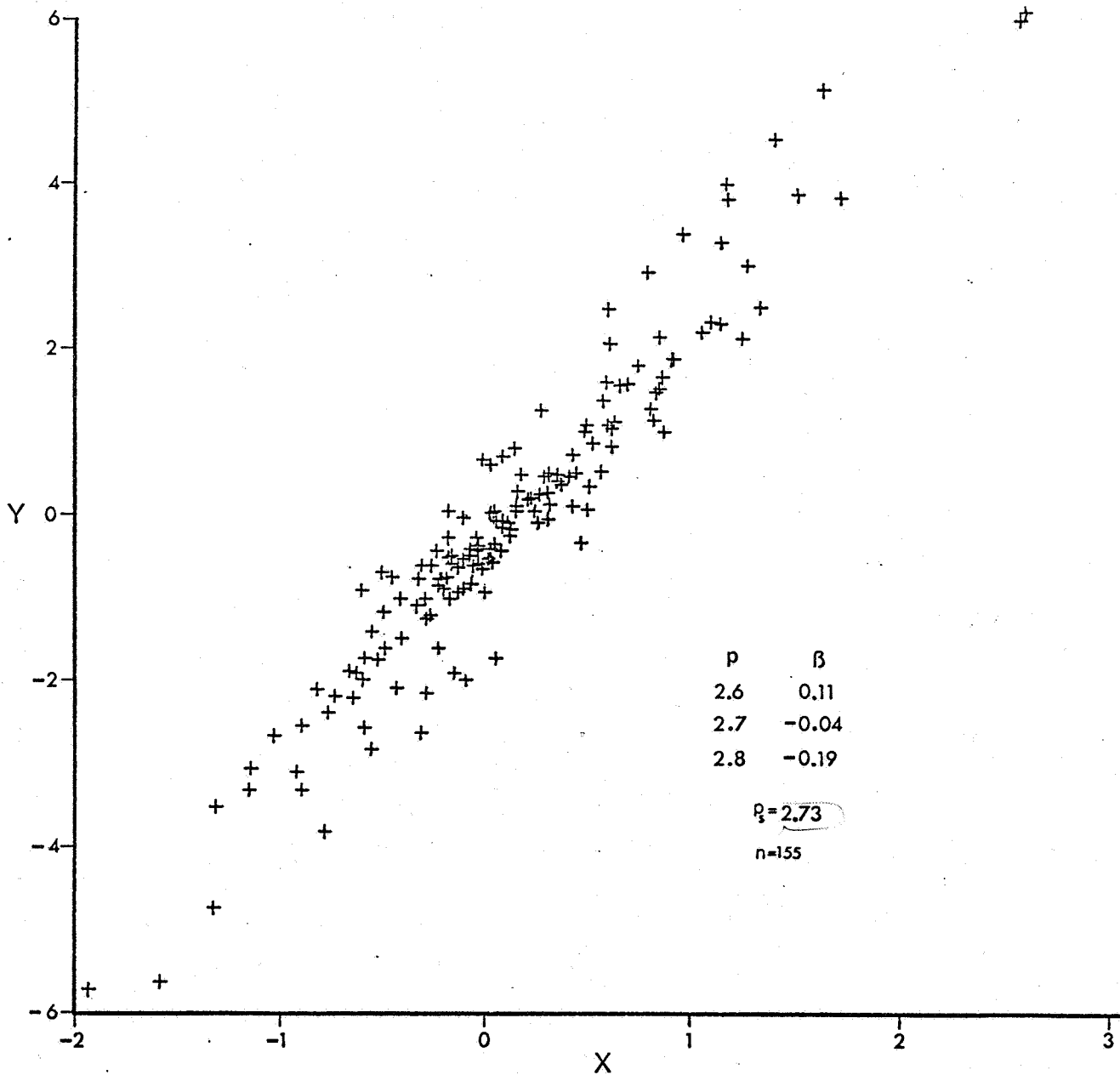
FIGURE 8

Indirect density determinations for Proterozoic
and Kanmantoo rocks.

agreement between the two methods. A comparison of the correlation coefficients in the two graphs shows how the regional removal has successfully removed a strong negative correlation between Bouguer Anomalies and topography.

Figures 7 and 8 show examples of solutions obtained (after regional removal) for the Proterozoic (Adelaidean) rocks, and for the inner portions of combined Kanmantoo and Proterozoic, respectively.

Densities for the Proterozoic (2.68 by the least-squares slope, 2.76 by the Density Profile method) suggest a figure around 2.72 g/cm^3. This is consistent with Tucker's estimate of a minimum 2.68 g/cm^3 for the Adelaidean unit. Kanmantoo Group rocks show a density of about 2.69 g/cm^3 which is slightly less than the 2.73 g/cm^3 given by Morony (SADM, 1971) for Kanmantoo metasediments of the Fleurieu Peninsula.

Over the combined Kanmantoo and Proterozoic, the best Bouguer density is suggested to be 2.71 g/cm^3. This is consistent with determinations for the individual members, and shows that the standard reduction density of 2.67 g/cm^3 is appropriate for the Ranges.

Measurements and observations over the Stonyfell Quartzite suggest a slightly higher density than the surrounding Proterozoic sediments, while it appears that the Palmer Granite is only very slightly less dense than the host Kanmantoo rock. Highs over the Rathjen Gneiss (Figure 2) suggest somewhat higher density than the Kanmantoo.

As mentioned previously, studies over the Archaean suggest that rock densities increase westward. This observation is supported by the fact that there is a significant anomaly at the western contact with the Proterozoic, but no significant anomaly (and, therefore, no significant density contrast) to the east near the Kitchener Fault. Denser rock types, for example, the Houghton diorite, also have been observed in the west (C. L. Horsfall, pers. comm.).

Table I summarises the densities adopted for various rock units involved in this study. The ranges quoted in the Table are not intended as indicators of accuracy or confidence limits; rather, they represent the ranges which were adopted for reduction and modelling in subsequent sections of this thesis. As seen from the Table, there are few "large" density differences between the major rock units, and this is evidenced by the rather undramatic residual Anomaly profiles.

TABLE I : DENSITY ESTIMATES

Unit	Adopted Density (g/cm^3)
Archaean (West)	2.80 – 2.90
Archaean (East)	2.72 – 2.80
Stonyfell Quartzite	2.72 – 2.76
Proterozoic	2.69 – 2.75
Rathjen Gneiss	(2.73)
Kanmantoo Group	2.67 – 2.72
Palmer Granite	2.66 – 2.69
Tertiary	2.20 – 2.30
Quaternary	2.14 – 2.20
Entire Profile	2.63
Kanmantoo + Proterozoic	2.71

IV. Regional-Residual Separation

Regional removal, as discussed at length in the literature, can be a subjective and largely arbitrary process. In the case of a two-dimensional profile (as at hand), the process is, nevertheless, fairly simple, and often the plausible alternatives are limited.

Plate I clearly shows that the Bouguer Anomaly consists of broad features and small superimposed anomalies. There are few "in-between" anomalies. This suggests that wavelength filtering might be suited here.

Wavelength filtering, using a moving average (or running mean) is a flexible and simple method to use, and as sound as far more elaborate techniques.

To perform this operation, the gravity data was first converted from its irregular spacing (313 points averaging 190m) and formatted into a 294-point profile at a regular spacing of 200m. This was achieved by using a form of cubic interpolation based on a published algorithm (Akima, 1972). All observed and calculated parameters were treated in this way, including free air and Bouguer Anomalies. To check accuracy, the latter were also recalculated from their interpolated components, and found to be consistent. Bouguer Anomalies were calculated for ten densities in the range 2.2 - 3.0, including 2.67.

Running means were applied to the interpolated Bouguer Anomalies, and a window of 5 km (25 equally-weighted points) was eventually chosen as the best filter.

Plate II shows the results of a regional removal from a 2.67 g/cm^3 Bouguer Anomaly profile. The bottom curve shows the original profile with the original stations marked by vertical strokes. Immediately above this is an upward continuation to 600 metres. Since upward continuation is strictly only applicable to stations on a plane, only the stations over the Range proper should be considered. (On the scale of the continuation, these stations may be regarded as on a plane at the average elevation of the Ranges - 360m). Accordingly, the loss of end-points in the continuation process is of no consequence.

Above the upward continuation is the wavelength-filtered curve, adopted as the regional. The similarity with the upward continuation confirms that broad features are involved. The regional curve has been extrapolated to cover the whole length of the traverse.

The fourth curve is the residual anomaly, obtained by subtracting the regional from the original Bouguer Anomaly curve.

The uppermost curve is the second vertical derivative of the original anomaly profile. Now, the second derivative is sensitive to localised fluctuations in a function, and therefore reacts to short wavelength anomalies. Accordingly, it would be expected to distinguish residual anomalies. Comparison to the curve below confirms this. The second derivative profile is also useful in interpreting step models (Bott, 1962) and was used in the Section on residual analysis. (To reduce noise, the second derivative was obtained from the interpolated data after it had been passed through a three-point binomial filter with weighting coefficients 0.15, 0.7, 0.15).

The 5-km window wavelength filtering method was applied to Bouguer Anomalies at all ten densities, as well as to free air anomalies and topography. Some of the relevant data is included in Appendix D.

Prior to evaluating residuals, the regional curves were interpolated to coincide with the original station positions. By doing this only the smooth regional itself carried errors of interpolation (which, by virtue of the smoothness were insignificant), and the residual was allowed to retain all its subtle characteristics.

For the sake of completeness, each regional was extrapolated to cover the whole traverse. In many cases, however, the extrapolation did not satisfactorily accommodate trends at the traverse edges. To illustrate this, Plate III shows residual topography (bottom, gravity stations marked) and residual Bouguer Anomalies at five densities. Anomaly F at 54.6 km appears similar in all profiles and appears to be associated with a 2 mgal high on its western flank. This "high" is, in fact, a rotational distortion due to the end-effects discussed above.

The western edge of the profiles has not suffered any appreciable end-effects, but it does contain an inaccuracy discovered late in interpretation. The elevations of the first two stations are in error, and the apparent westward climb of the anomaly over these stations is incorrect.

The use of residuals in density determinations has already been described, and in the following sections the interpretation of regional and residual Bouguer Anomalies is discussed.

V.   Regional Analysis

In this section, the wavelength-filtered regional calculated at 2.67 g/cm³ and shown in Plate II is analysed. Preliminary comments on regional aspects of the profile and two adjacent profiles were made earlier in relation to Figure 3.

A striking feature of the regional is that a central low (-16 mgal) is flanked symmetrically by two shoulders which rise some 4 mgal above the broader trend. These shoulders are too broad to be classed purely as residual anomalies, and are discussed shortly.

From the central low, the anomaly rises until, at the edge of the Ranges, it falls off again. Our attention will at present be confined to the anomaly over the Range proper between chainages 5-40 km. Over this section, the Northern profile of Figure 3 is similar, although the shoulders are less pronounced, and the Southern profile is only similar in its western half. The central low, in all three profiles, is displaced roughly 10 km east of the geographic centre of the Ranges. An asymmetry, in the form of an eastward fall of the anomaly, is also common to all three profiles.

Figure 4 shows the broad correlation between the regional trends of elevation and Bouguer Anomaly. This inverse relation is usually associated with crustal thickening below mountain and hill ranges, and is the basis of many empirical depth-to-Moho calculations (Woollard, 1959).

Accordingly, it is desirable that the gravitational effect of postulated crustal thickening should be investigated. In order to establish an initial model, it is necessary to have some idea of the normal crustal thickness flanking the Ranges, and also an indication of what sort of thickening might be plausible under them.

To this end, the data from this survey was employed in the empirical methods of Woollard (1959) and combined with other geophysical evidence, to determine an estimate of the Moho depth in the vicinity of the Ranges. For an initial estimate of thickening involved, theoretical calculations by Mumme (1961) for "mountain roots" of an Airy isostatical model were used. The calculations are outlined in Appendix C, and yield a normal thickness of 36 km and a 2 km depression of the Moho under the Ranges.

Using this as a starting model, several configurations of crustal thickening were examined for their gravitational effect. For this purpose, a computer programme written by the author (based on the two-dimensional polygonal method of Morgan and Grant, 1963) was used.

In these model studies, attempts were made to duplicate the shoulders of the regional profile. It was found that, in order to match the sharpness of the anomalies, no plausible model could achieve this duplication. These anomalies cannot, therefore, be solely due to any structures postulated at Moho depths.

Numerous models suggest that the configuration which comes closest to describing the three regionals of Figure 3, can only be achieved by assuming that the crust thickens asymmetrically eastwards under the Ranges. This displaces the minimum east of the geographic centre and results in a slightly asymmetrical profile.

A model fitting this description (in broad terms) is shown in Figure 9, together with its theoretical Bouguer Anomaly (solid line) and the observed regional (marked by crosses at each fifteenth station over the Range proper). The mantle is assumed to be 0.55 g/cm^3 denser than the crust. It should be emphasized that this model is not really an attempt to "fit" the regional, but is more an attempt to show what anomaly might be expected purely from a crustal thickening.

According to the model of Figure 9, a crustal thickening (or depression of the Moho) of the order of 3 km or more (depending on the shape of the thickening) would give rise to regionals not inconsistent with those observed. The model assumes that a state of equilibrium exists, or nearly does so.

(If an isostatical model is assumed, compensation over large areas is indicated by a free air anomaly approaching zero in central portions. This point was alluded to in a discussion of Figure 4 where it was noted that the free air anomaly remains quite flat. Even if an isostatical model was seriously considered, however, the area involved is too narrow to draw any conclusions along these lines).

The shoulders discussed earlier in this section were examined by maximum-depth rules (Smith, 1959) and by rough models. It is difficult to envisage any near-surface geophysical model which could account for these anomalies and at the same time fit observed geology. As has been mentioned, structures at Moho depths cannot (alone) account for them.
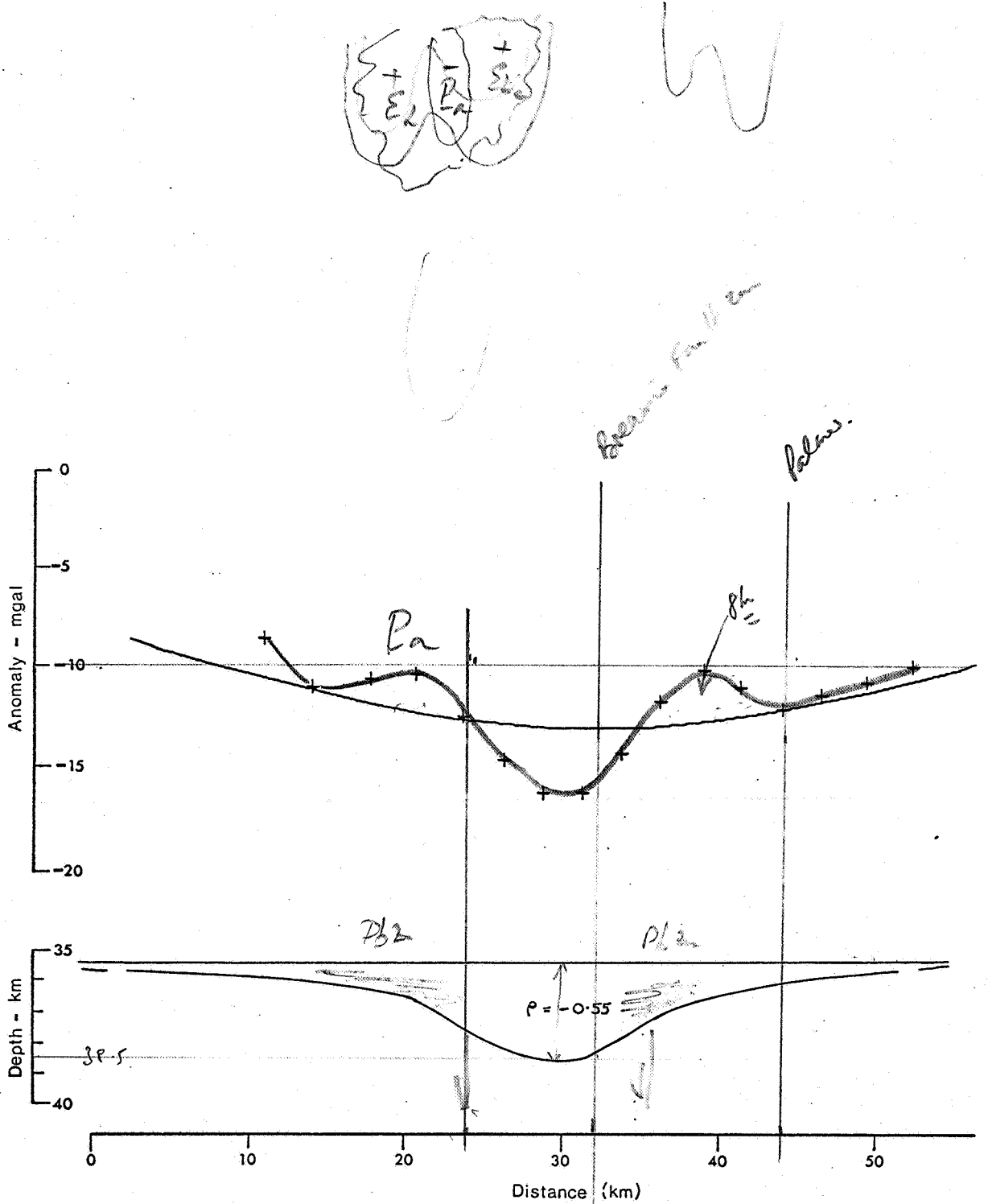
FIGURE 9

Crosses mark the observed Bouguer Anomaly every fifteenth
station across the central part of the Ranges. The solid
line represents the theoretical anomaly for the anomalous
mass shown below, which is a model for crustal thickening
under the Ranges. Bouguer Anomalies are absolute.   Only
slight asymmetry is shown here.
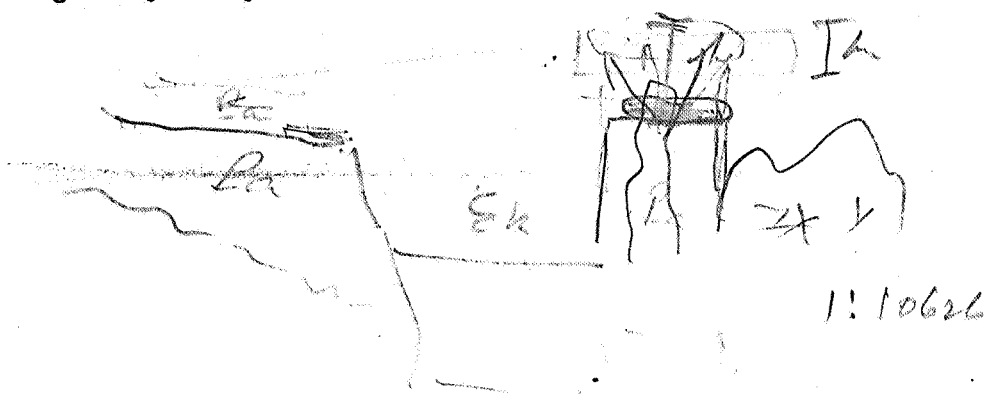
It does appear, however, that they are primarily due to density contrasts within the upper 10 km of the crust, and a variety of basement structures can be found to produce anomalies of the required shape and size. For example, anomalous masses with two-dimensional cross-sections of a few square kilometres, at contrasts of about 0.2 g/cm^3, and depths of about 8 km, are easily capable of producing such anomalies.

It is pointless to suggest any more detailed model without some form of control.

VI.   Residual Analysis

The residuals shown in Plate III demonstrate that the profile is reasonably featureless. Total relief is less than 10 mgal, and most fluctuations are only of the order of 1 mgal. Small errors normally tolerable in other surveys become significant, and extreme care is needed in deciding whether a particular "anomaly" is genuine or might be the result of small errors in one, or perhaps two, stations. The effect of topography must be carefully scrutinised as well.

The lower profile in Plate III shows the residual topography (gravity stations marked). A schematic summary of known geology is also marked.

Starting at the western end of the profile, a complex anomaly pattern emerges over the Eden Fault and the Archaean-Proterozoic boundary. In Section IV it was noted that some distortion occurs at the edges of the profile, and also that the first two stations should be neglected.

Reference to Plate I clearly shows that the choice of density profoundly affects this anomaly pattern. At a density of 2.2 g/cm^3 there is a small high over the Stonyfell Quartzite and a 7.5 mgal drop over the Eden Fault. At a density of 3.0 g/cm^3 there is a large high over the Quartzite and a 3.0 mgal drop over the Fault.

The anomaly pattern is best considered at different densities for its two components. (A over the Eden Fault and B over the Archaean fault-boundary). For anomaly B, a density of 2.8 has been selected for study, since it involves the high density rocks of the western Archaean and the Proterozoic. As the anomaly falls to a flat-bottomed low on its western flank, values start to rise again over the Stonyfell Quartzite. The Quartzite is not, however, much denser than its surrounds, and it is suggested that there is a thickness of lower density material associated with the fault-boundary which helps contribute to the adjacent highs. Over Anomaly A, a lower density of 2.4 g/cm^3 has been used to best describe the Tertiary and Proterozoic rocks. This results in a 6.7 mgal drop across the Eden Fault.

The anomalies A and B, separated in this way, are examined in more detail later in this Section.

Over the Archaean, values fall steadily towards the east, and it
has been noted that rock densities appear to fall in this direction.
A small high (Anomaly C1) may be due to a small area of higher-density
Archaean rock.

At the position of the Kitchener Fault, a small 0.4 mgal drop
occurs as Proterozoic rocks begin outcropping. In view of the
comparative size of adjacent fluctuations, it is impossible to say
whether or not this is an expression of the Fault, and it appears
that the Bouguer Anomaly profile is smooth across this boundary.

Over the Proterozoic, the anomaly pattern shows some fluctuation,
but an inspection of the topography reveals that these "anomalies"
are closely related to the terrain (Plate III) and are not interpreted
beyond this.

A small high (Anomaly C2), not apparently correlated with topography,
is associated with a small fault running along its eastern margin. An
interpretation, however, could not be offered.

Values drop steadily as the Proterozoic-Kanmantoo boundary is
crossed eastwardly, but no anomaly is observed over the contact.

Over the Kanmantoo, the anomaly pattern is very featureless. A
small low, some 3 km wide, occurs over some Quaternary sediments on
the western margin of the Bremer Fault Zone. Values increase slightly
to the east over an area of fold axes and outcropping amphibolites and
gneisses; a sharp 1.7 mgal anomaly (D) appears to offer the most
promise for interpretation, and is shortly discussed.

At low densities (see Plate III) Anomaly D appears to be superimposed
on a broader high, but at more appropriate densities (2.6 - 2.8) the
background is fairly flat.

Over the eastern edge of the Ranges, the anomaly profile remains
fairly flat, and only a small low of 1.1 mgal is associated with the
Palmer Fault (Anomaly E). Anomaly values increase quickly east,
suggesting only thin sediment infill; this is likely in view of the
outcrops of Kanmantoo, and granitic and gneissic rocks. Some of these
rocks (the gneisses?) may be slightly denser than surrounding rocks,
and small highs occur over them.

At the 52 km mark, distortion affects the residual profiles (as mentioned in Section IV). The profiles actually remain quite flat until, at 54.6 km, a 5.6 mgal anomaly (F) marks a boundary between granites and a thickness of Murray Basin sediments.

Interpretation by computer modelling was based on two programmes written by the author.* The first, which was mentioned in the previous Section, is based on Talwani's polygonal algorithm as modified by Morgan and Grant (1963), and calculates the gravitational effect of an anomalous mass approximated by a two-dimensional polygonal body. The programme allows for the effect of an uneven level of observation, provided the anomalous mass is everywhere below it. The other programme is based on the step model of Grant and West (1965, p.283). (It should be noted that the formula given there, as it stands, is dimensionally ambiguous). In addition, the method of second derivatives (Bott, 1962) was also used to help deduce the direction of the sloping face for various step models.

Although all the observed anomalies are small, the close spacing of the stations made quantitative interpretations possible on the anomalies A, B, D, E and F.

---

* It is hoped to generalise these programmes and lodge details with the Department of Economic Geology, University of Adelaide.

Anomaly A

At a density of 2.4 g/cm^3, the anomaly over the Eden Fault measures 6.7 mgal and represents a contrast between Proterozoic (Stonyfell Quartzite) and Tertiary rock.

A simple step model, density contrast 0.55 g/cm^3, was assumed. Allowing for the change in elevation across the scarp the anomaly is consistent with an anomalous thickness of 150m.

The best model fit indicated a near vertical fault, perhaps dipping slightly to the west. The anomaly is here interpreted as an 80-85° W dip of the Eden Fault with a Tertiary thickness of some 150 metres.

Anomaly B

At a density of 2.8 g/cm^3, anomaly B measures 5.8 mgal and represents the (fault) boundary between the western part of the Archaean, and the Proterozoic, near chainage 4.3 km.

Assuming the Archaean to be 0.10-0.30 mgal denser than the Proterozoic, and the level of observation to be a horizontal plane, several step model configurations were tested against the anomaly.

These models clearly showed that an easterly dipping boundary was implied.

At a contrast of 0.15 g/cm^3 the anomalous mass must exceed 1 km in thickness, while at 0.30 g/cm^3 a thickness nearer 0.5 km would be implied. Although the former contrast is felt more appropriate, large movements along the fault would be suggested.

Figure 10 shows the observed anomaly (marked by crosses at 200m interpolated positions) and two computer models. The solid line (Model I) represents a 35°E fault at contrast 0.28 g/cm^3 and thickness 550m. The dotted line (Model II) represents a 70°E fault, contrast 0.15 g/cm^3, thickness 1.3 km. The theoretical positions of the fault corresponding to the models are 4.2 km (I) and 4.4 km (II).

FIGURE 10

Anomaly B (crosses) compared with computer models I and II
(solid and dotted lines respectively). Model I incorporates
a flat regional of -13·3 mgal, model II -14·1 mgal, for
step model computations.
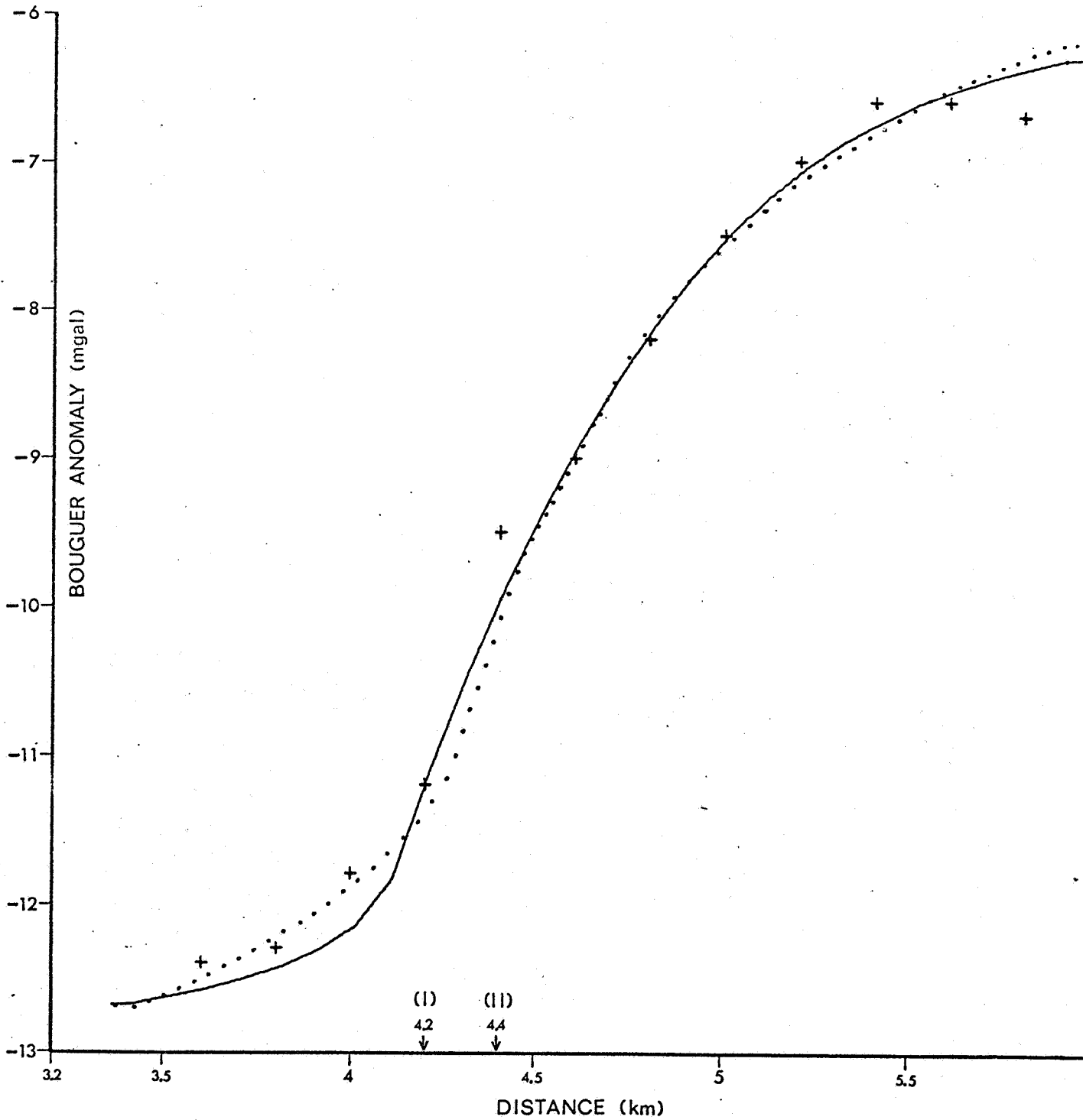
Other factors must also be considered in the interpretation.
Firstly, if - as has already been suggested - there is a thickness
of low-density material on the western flank of the fault, then the
size of the true anomaly has been overestimated. Secondly, checks on
the original data suggest that terrain corrections in Zones E-G are
uncertain. Lastly, the models shown in Figure 10 possess slightly
greater amplitudes than the observed anomaly (in order to match the
central parts of it).

With these points in mind, the following tentative interpretation
is put forward. The boundary is easterly dipping, at about 60°, and,
assuming a contrast of 0.15 g/cm³, the displacement along the fault
is less than, but of the order of, one kilometre.

Anomaly D

At 40.6 km a sharp-peaked anomaly of half-width 420m occurs. The
anomaly does not coincide with any mapped surface geological feature,
and attempts were therefore made to discover what type of body might
be responsible.

The shape of the anomaly suggests a spherical model, and its
half-width implies the depth to the centre would be about 250-300m.
Preliminary calculations showed that a two-dimensional flat-topped
body would be more appropriate. Bodies varying from a cross-sectional
semi-circle to a more depth-extensive body were modelled. Depending
on assumed density contrasts, a variety of these models met with
similar degrees of success, but lack of other geophysical control did
not justify favouring any one model. For example, a two-dimensional
rectangular body 500 x 100m, under 25m of cover (contrast 0.6 g/cm³),
or a steep dyke-like body of contrast 0.1 g/cm³, might produce the
required effect.

It is suggested that further investigation of this particular
anomaly might profitably yield a more definitive interpretation. The
models discussed above are not inconsistent with mineralization.

Anomaly E

The Palmer Fault (43.8 km) coincides with a small 1.1 mgal
anomaly. Since the adjacent noise level is also of this magnitude,
any interpretation must be treated with a certain amount of caution.

Although the anomaly is really only defined by three points, second derivative studies suggest that the fault is approximately vertical.

Assuming that the contrast between Kanmantoo Group rocks and Quaternary sediments is 0.5 g/cm^3, a 40 metre displacement is suggested (after elevation has been taken into account across the fault).

Accordingly, the anomaly is interpreted as that due to a near vertical 40 metre displacement of the Palmer Fault.

Anomaly F

A boundary between granites and Murray Basin sediments is indicated at chainage 54.6 km by a 5.6 mgal anomaly. This is interpreted as a fault-like truncation of granitic rock (0.5 mgal denser than adjacent Quaternary sediment) dipping at 50°E and extending to a depth of about 280m.

Figure 11 shows a comparison of the observed anomaly (actual points marked by crosses) with the above interpretation (solid line).

Although the depth indicated is deeper than might be suggested by bores a short distance away (about 150 metres), there is little room for an alternative model to fit this well-defined anomaly. Gravity values appear to increase again to the east, and the interpreted depth may only apply in the vicinity of the inferred contact.
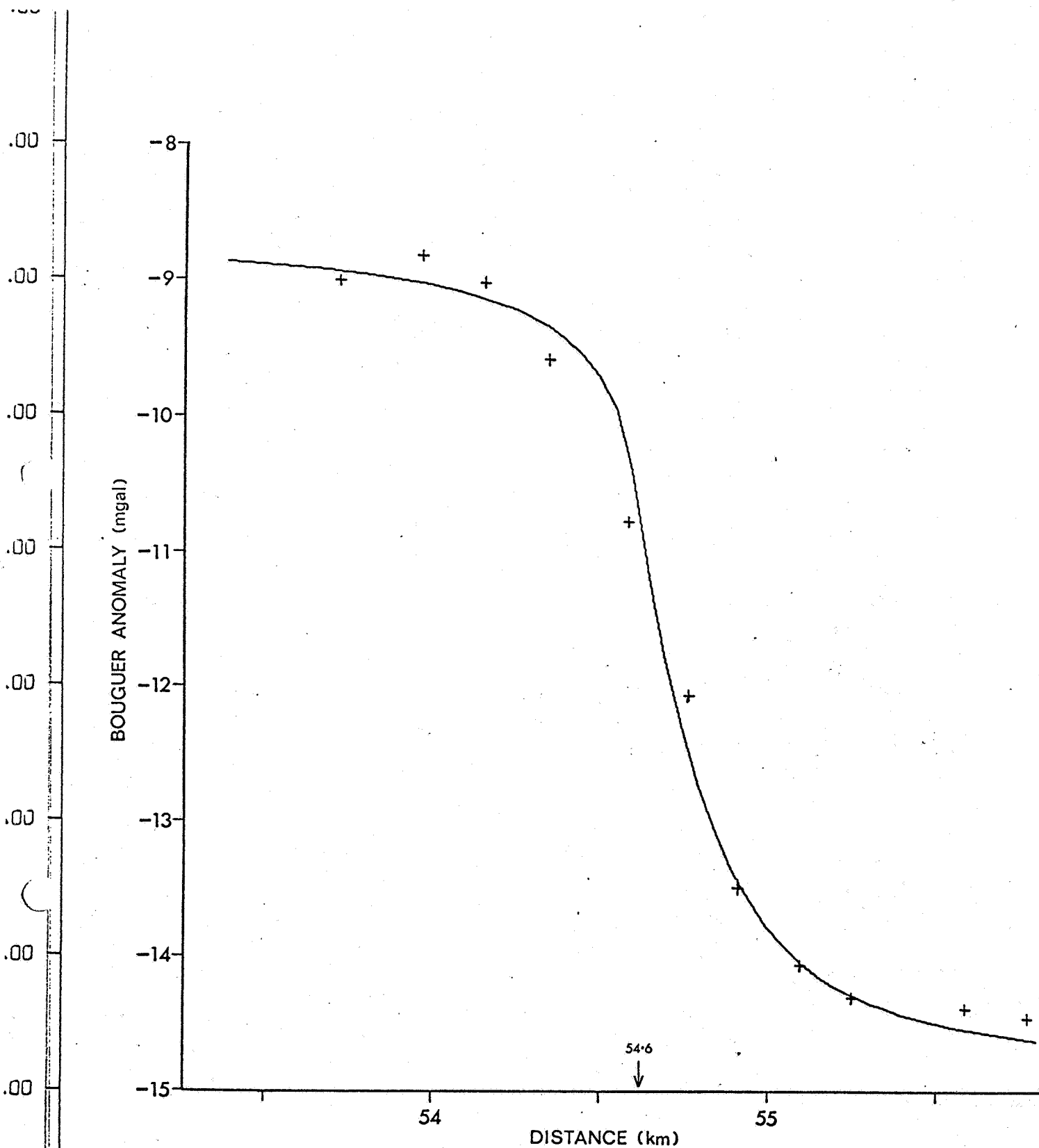
FIGURE 11

Anomaly F (crosses) and its interpretational model
(solid curve). Flat computational regional, -8·7 mgal.

Conclusions

The survey described herein has been useful in delineating some broad and local features of the central Mt. Lofty Ranges and is suited to future follow-up work. This work would include co-ordination with other geophysical techniques, not possible in this short study.

Indirect density measurements were shown to be a valuable adjunct in deciding on suitable densities for reduction and geophysical models, providing the following conditions are satisfied:-

(i) There is a high station-density over the relevant rock units.

(ii) There is appreciable topographical relief over each unit (after removal of a smooth regional surface).

(iii) Regional topography and regional anomalies have been removed, or may be assumed flat, or, in some cases, appear to be "balanced".

(iv) Genuine anomalies are sufficiently "random" over the area examined.

If the methods of Nettleton (1939) and Parasnis (1962) are not in substantial agreement, it is likely that the above conditions have not been satisfied. A variety of determinations should be made for each unit, by suitable station choices.

Indirect measurements aided in compiling a table of densities for rocks encountered in the survey (Table I).

Of special note is that Archaean rocks appear to become denser westward.

Preliminary examinations of the regional Bouguer Anomaly over the Ranges indicate that the crust may asymmetrically thicken eastward to a depth of 39 km, from a normal thickness of 36 km on the Range flanks. Also, basement structures may possibly be indicated in the regional gravity picture.

The residual gravity anomaly is a rather featureless profile, reflecting the lack of large density contrasts existing over the Ranges. Quantitative interpretations proved possible in a few cases, summarised as follows:-

(i)   The Eden Fault dips 80-85° W with a displacement of 150m.

(ii)   The boundary between the Archaean and Proterozoic in the western part of the Ranges is a fault dipping about 60°E, and involves a displacement approaching 1 km.

(iii)   The Palmer Fault is near-vertical, and shows a 40m displacement.

(iv)   A fault-like truncation of Palmer Granite occurs at chainage 54.6 km, where the granite boundary dips 50°E against 280m of Quaternary sediments.

(v)   A small 1.7 mgal sharp-peaked anomaly (chainage 40.6 km) needs further investigation before a reliable interpretation can be advanced.

Similar profiles must be carried out along parallel traverses before confirmation of these interpretations is possible, and there is definite need to integrate data from other geophysical techniques (for example, aeromagnetics).

References

(Cited in the text and appendices)

Akima, H., 1972. Interpolation and smooth curve fitting based on local procedures. Algorithm 433, Comm. Assoc. Comp. Mach. 15: 914-918.

Bott, M.H.P., 1962. A simple criterion for interpreting negative gravity anomalies. Geophysics 27: 376-381.

Doyle, H.A., and Everingham, I.B., 1964. Seismic velocities and crustal structure in southern Australia. Geol. Soc. of Aust. Jour. 11: 141-150.

Grant, F.S., and Elsaharty, A.F., 1962. Bouguer corrections using a variable density. Geophysics 27: 616-626.

Grant, F.S., and West, G.F., 1965. Interpretation theory in applied geophysics (McGraw-Hill): 243-250, 282-287.

Hammer, S., 1939. Terrain corrections for gravimeter stations. Geophysics 4: 184-194.

Heiskanen, W.A., and Vening Meinesz, F.A., 1958. The Earth and its gravity field (McGraw-Hill): 201-210.

Morony, 1971. SADM unpublished data.

Morgan, N.A., and Grant, F.S., 1963. High speed calculation of gravity and magnetic profiles across two-dimensional bodies having arbitrary cross-section. Geophys. Prosp. 11: 10-15.

Mumme, I.A., 1960. Determination of the crustal thickness of the Earth in the general region of Adelaide, South Australia. Trans. Roy. Soc. S.A. 84: 61-62.

Mumme, I.A., 1961. Isostatic study of the Mount Lofty Ranges, South Australia (unpublished).

Nettleton, L.L., 1939. Determination of density for reduction of gravimeter observations. Geophysics 4: 176-183.

Parasnis, D.S., 1962. Principles of applied geophysics (Chapman and Hall): 39-41.

Sandberg, C.H., 1958. Terrain corrections for an inclined plane in gravity computations. Geophysics 23: 701-711.

Smith, R.A., 1959. Some depth formulae for local magnetic and
    gravity anomalies. Geophys. Prosp. 7: 57.

Tucker, D.H., and Brown, F.W.,1973. Reconnaissance helicopter
    gravity survey in the Flinders Ranges, South Australia,
    1970. Bur. Min. Res. Geol. and Geophys. Record 1973/12.

Vajk, R., 1956. Bouguer corrections with varying surface
    density. Geophysics 21: 1004-1020.

White, R.E., 1969. Seismic phases recorded in South Australia
    and their relation to crustal structure. Geophys. J.R.
    astr.soc. 17: 249-261.

Woollard, G.P., 1959. Crustal structure from gravity and
    seismic measurements. Jour. Geophys. Res. 64: 1521-1544.

Also consulted during the preparation of the thesis:-

    Smith, L.F. (Ed.) 1972. The Australian Metric Manual
        (West); and also current Schedules under
        Section 3 of the Australian Metric Conversion Act,
        1970-71.

    Tidal Gravity Corrections for 1973: Geophysical Prospecting
        Supplement.

APPENDICES

APPENDIX A : Effect of the Pipeline

For the purposes of a simple theoretical calculation, the mass of the pipeline may be regarded as concentrated in a thin, infinite line. The corresponding linear density of such a line is estimated to vary between 200 and 1200 Mtex*, depending on the pipe's water content.

The gravitational effect of such a line element, about 1 metre above a ground station, is less than the order of 0.01 mgal.

Other theoretical calculations were made by assuming simple shapes and using computer models to evaluate them, and also by calculating an "equivalent" terrain correction. These calculations confirmed the above observation.

Field measurements also failed to detect the presence of the pipeline.

As final verification, it should be noted that several stations were made over bench marks some distance from the pipeline. Reduced data from these stations shows complete continuity with data from stations made close to the pipeline.

---

* 1 megatex (Mtex) $= 1 \text{ kg.m}^{-1}$

APPENDIX B : Data Accuracy

Errors in the Bouguer Anomaly arise from inaccuracies in
latitude and elevation control, instrument drift, and, lastly,
terrain corrections.

Latitude

The tables given in Appendix D quote latitudes to 0.01 degrees.
The nature of their determination does not permit this degree of
accuracy in the absolute sense. Over small distances of a few
kilometres, however, the relative accuracy is estimated at 0.02°.
The absolute latitude is estimated accurate to $\pm 0.05^\circ$.

Since we are really only interested in relative latitudes over
a smoothly continuous profile, the maximum error from this source
is probably 0.02°, or 0.03 mgal.

Elevation

The text describes the procedure adopted for locating stations
of determinable elevation (p.4). The accuracy of fixing a horizontal
position on the pipeline was estimated to be better than 1 metre.
After determining a ground elevation from the underside of the pipe,
at that point, the elevation was estimated to be within $\pm$ 20 cm
of the true ground level.

This corresponds to an uncertainty of 0.04 mgal.

Drift

Variations in the gravimeter factor, earth-tide, and operator
errors contribute towards the quantity known as drift. Drift
manifests itself on the form of miss-ties and non-repeatability.

Theoretical calculations were made to remove the effects of
earth-tide, and resultant drift was nearly always better than $\pm$ 0.03
mgal, (p.5), and was usually $\pm$ 0.02 mgal.

The normal summary error in Bouguer Anomalies corresponding to these uncertainties is given by

$$(0.03^2 + 0.04^2 + 0.02^2)^{\frac{1}{2}} = \pm 0.05 \text{ mgal}$$

The evaluation of terrain corrections was carried out to the degree of accuracy possible for the method, and corrections are, therefore, better than 0.1 mgal (Hammer, 1939). (Hammer's estimate applied to larger corrections than were involved here).

From the above uncertainties, the Theory of Errors predicts that a given Bouguer Anomaly value will be accurate to $\pm$ 0.10 mgal. It is felt that the maximum likely error is probably less than this.

It might be said that an uncertainty of 0.1 mgal makes a station spacing of 190 metres somewhat redundant. The relative accuracy is probably much better than this; and, in any event, all commercial surveys aim for this same accuracy. In addition, of course, close spacing can avoid later re-runs, and allows simple filtering to be used to advantage without loss of information.

Two points should be mentioned before leaving the topic of data accuracy. The first is that the elevation of the first two stations (AH001 and AH002) is uncertain, and these points (at the western extremity) should be neglected. The second point concerns the end-effect distortions introduced by regional removal, and this is fully discussed in the main text (pp 15-16).

APPENDIX C : Depth to the Moho

The empirical methods of Woollard (1959) use parameters of elevation and Bouguer Anomaly to determine depth to the M-discontinuity. The methods use the absolute anomaly, calculated at 2.67 g/cm^3, and assume equilibrium conditions exist.

It should be quite obvious that these empirical methods are subject to large uncertainties, but it is nevertheless instructive to apply them.

In order to define an "average" anomaly and elevation, the Range was defined at the 250m contour (Australian Height Datum). An analysis was then made of the corresponding profile data. For this purpose the regularly-spaced interpolated data was used.

In evaluating an average elevation, use was also made of digitized elevation charts prepared for evaluating terrain corrections. (Topography was digitized in 1000-yard squares). A ten-kilometre band was considered, with the pipeline along its axis. The mean elevation determined from this was averaged with the mean determined from the profile data. Bouguer and free air anomaly averages were obtained solely from the profile.

The results obtained are summarised as follows:-

> Mean Range elevation: 360m   (st.dev.90m)
> Mean Bouguer Anomaly: -10.7 mgal (st.dev.4 mgal)
> Mean free air anomaly: 30.0 mgal (st.dev.7.6 mgal)

The relevant computations are described below.

(a) Applying Andreev's formula:

$$M = 0.1\Delta g + M_o$$

where M is the depth to the Moho (km), Δg is the Bouguer Anomaly (mgal), and Mo is the "normal" (Australian) crustal thickness (assumed as 33 km), we obtain a value of 32 km.

(b)   Applying Woollard's relation between elevation and crustal thickness (Woollard, 1959, p.1532), a value of 34 km is obtained.

(c)   Applying Woollard's relation between Bouguer Anomaly and crustal thickness (Woollard, 1959, Fig.8), a value of 33 km is obtained.

(d)   Applying an equation used by Russian and Chinese seismologists,

$$M = 33 \tanh (0.38\Delta h - 0.18) + 38.0$$

where Δh is the elevation (km), we obtain a value of 37 km.

(e)   Applying another equation used by Russian and Chinese seismologists, relating Bouguer Anomaly to crustal thickness,

$$M = 35 (1 + \tanh 0.0037\Delta g)$$

where Δg is the Bouguer Anomaly, a value of 36.5 km is obtained.

(f)   Applying Heiskanen's and Vening Meinesz's formula (Heiskanen and Vening Meinesz, 1958)

$$M = M_0 + 6\Delta h$$

where Δh is the elevation (km), and M_0 is assumed to be 33 km, a value of 35 km is obtained.

Averaging all the above results yields a value of 35 km for the crustal thickness under the Ranges.

In seismic studies of Southern Australia, Doyle and Everingham (1964) state that "no simple correlation occurs between .... gravity values and the estimates of crustal thickness" (p.149), but the results determined above are in reasonable agreement with the results quoted by these authors and also by Mumme (1960) and White (1969).

The more recent of these publications indicate slightly higher crustal thicknesses for the area, and Stewart (pers.comm.) feels that a figure of 37 km would be more appropriate.

With all this information, a figure of 36 km was selected as the normal crustal thickness _flanking_ the Ranges.

In order to obtain an estimate of "plausible" crustal thickening under the Ranges, calculations by Mumme (1961) were used. He assumed an Airy isostatic model was operating and calculated a "mountain root" by applying Archimede's Principle. He assumed that the normal Moho depth for the neighbouring Plains was 33 km, and that the Range width was 35 km at an average 300m elevation. His calculated mountain root was 1.8 km. In the present situation, the Range width is 37 km at an average 360m elevation, and the neighbouring Plains have an assumed 36 km crust. A slightly larger "root" would therefore be implied, and a figure of 2 km is suggested as an initial estimate for crustal thickening under the Ranges.

APPENDIX D : Selected Data Tables

    After field collection of data, processing was done both manually
and automatically, as discussed in Section I of the text. Initially,
techniques of tidal drift and instrument drift corrections were applied,
and adjustments were made to base networks and so on. The production
of "Observed Gravity" in milligals, for each station, was a manual
process.

    The data was then collated and put on to punched cards. The
data was operated on and, after further processing, was arranged
into five cycles of a permanent disk-file. Information stored on
these cycles included raw material, free air and Bouguer Anomalies
(at various densities), and regularly-formatted interpolated data,
as well as comprehensive regional curves.

    This arrangement of stored data saved inefficient re-calculation
of fundamental parameters, as well as allowing multiple access to a
convenient set of data.

    Some of the data stored on the permanent file is reproduced here.
From it, any of the calculations used in the text may be duplicated.
(The full file contents have been lodged with the Department of
Economic Geology).

    It will be noted that "Chainages" are listed on two orientations.
The first, using Imperial notation, runs from east to west. This
conforms with the "as constructed" E & WS Plans of the pipeline. The
metric chainages adopted in this thesis run from west to east. The
metric chainage is related to the Imperial chainage by the equation

$$M = 0.3048 (195479 - C)$$

where M is the metric chainage in metres and C is the Imperial
chainage in feet.

    There are three different elevations listed. The abbreviations
are here explained as follows:-

(1) R.L. This is the "reduced level" used by the E & WS for
     construction of the pipeline and for old benchmarks. The
     datum involved is 105.68 feet below Mean Sea Level, Port
     Adelaide. This datum was adopted to avoid negative elevations.

(2) <u>A.H.D.</u>   This is the new Australian Height Datum, adopted in 1972 as the metric "sea-level" for the whole Australian continent.

(3) <u>MSLPA</u>   (Mean Sea Level, Port Adelaide). This is the old South Australian height datum.

STATION	CHAINAGE (E-W) MILES	FEET	(W-E) METRES	LATITUDE DEG	MIN	ELEVATION R.L. (FEET)	A.H.D. (METRES)	MSLPA (FEET)	TERRAIN CORRECTIONS (MGAL) 2.0	2.67	OBSERVED GRAVITY (MGAL)
AH001	36	4560	274	34	50.59	689.00	177.55	583.32	.25	.33	687.31
AH002	36	2325	1028	34	50.50	776.35	204.17	670.67	.41	.55	680.69
AH003	36	898	1371	34	50.41	841.00	223.88	735.32	.57	.76	675.31
AH004	36	242	1571	34	50.34	851.25	227.00	745.57	.76	1.01	675.04
AH005	36	8	1643	34	50.34	845.73	225.32	740.05	.92	1.23	675.45
AH006	35	5040	1718	34	50.36	837.50	222.81	731.82	.78	1.04	675.94
AH007	35	4405	1912	34	50.38	910.63	245.10	804.95	.86	1.15	671.87
AH008	35	3980	2041	34	50.42	999.25	272.11	893.57	.84	1.12	667.98
AH009	35	3605	2156	34	50.43	1103.73	303.96	998.05	.89	1.19	662.48
AH010	35	3410	2215	34	50.46	1158.00	320.50	1052.32	.84	1.12	659.87
AH011	35	2760	2413	34	50.52	1184.66	328.62	1078.98	.67	.89	659.20
AH012	35	2405	2521	34	50.53	1198.54	332.85	1092.86	.77	1.03	658.67
AH013	35	2205	2582	34	50.55	1225.08	340.94	1119.40	.77	1.03	657.06
AH014	35	1755	2720	34	50.54	1317.55	369.13	1211.87	.74	.99	651.52
AH015	35	1375	2835	34	50.53	1354.65	380.44	1248.97	.83	1.11	648.23
AH016	35	955	2963	34	50.53	1282.00	358.29	1176.32	.87	1.16	652.57
AH017	35	724	3034	34	50.53	1303.40	364.82	1197.72	.97	1.29	650.96
AH018	35	400	3133	34	50.53	1323.20	370.85	1217.52	.92	1.23	649.90
AH019	35	100	3224	34	50.53	1362.76	382.91	1257.08	.94	1.25	647.29
AH020	34	4550	3477	34	50.46	1464.86	414.03	1359.18	.76	1.01	639.40
AH021	34	3410	3824	34	50.41	1365.14	383.63	1259.46	.39	.52	645.66
AH022	34	3210	3885	34	50.40	1355.10	380.57	1249.42	.38	.51	646.33
AH023	34	2810	4007	34	50.39	1341.17	376.33	1235.49	.36	.48	647.52
AH024	34	2535	4091	34	50.39	1356.33	380.95	1250.65	.25	.33	646.87
AH025	34	2310	4160	34	50.39	1348.33	378.51	1242.65	.17	.23	647.77
AH026	34	1885	4289	34	50.39	1336.34	374.86	1230.66	.18	.24	649.28
AH027	34	1485	4411	34	50.38	1329.27	372.70	1223.59	.24	.32	650.82
AH028	34	1210	4495	34	50.38	1339.19	375.72	1233.51	.18	.24	650.78
AH029	34	1010	4556	34	50.38	1363.56	383.15	1257.88	.32	.43	648.96
AH030	33	4592	5074	34	50.39	1388.80	390.85	1283.12	.26	.35	649.50
AH031	33	3955	5268	34	50.39	1374.25	386.41	1268.57	.26	.35	650.84
AH032	33	3663	5357	34	50.39	1378.42	387.68	1272.74	.22	.29	650.81
AH033	33	2613	5677	34	50.38	1387.38	390.41	1281.70	.20	.27	650.67
AH034	33	2013	5860	34	50.37	1393.51	392.28	1287.83	.18	.24	650.42
AH035	33	1613	5982	34	50.37	1376.65	387.14	1270.97	.14	.19	651.49
AH036	33	1213	6103	34	50.36	1364.20	383.35	1258.52	.19	.25	652.38
AH037	33	613	6286	34	50.35	1401.89	394.84	1296.21	.14	.19	649.81
AH038	33	415	6347	34	50.36	1402.60	395.05	1296.92	.20	.27	649.76
AH039	32	5039	6547	34	50.36	1334.88	374.41	1229.20	.17	.23	653.93
AH040	32	4213	6798	34	50.35	1369.61	385.00	1263.93	.14	.19	651.50
AH041	32	3400	7046	34	50.33	1295.25	362.33	1189.57	.19	.25	655.97
AH042	32	2768	7233	34	50.35	1317.34	369.06	1211.66	.14	.19	654.43
AH043	32	2230	7397	34	50.35	1340.87	376.24	1235.19	.17	.23	653.02
AH044	32	1670	7572	34	50.35	1386.93	390.28	1281.25	.18	.24	649.74
AH045	32	1063	7758	34	50.32	1415.81	399.08	1310.13	.62	.83	647.74
AH046	32	900	7808	34	50.19	1437.40	405.66	1331.72	.24	.32	646.40
AH047	31	5000	8168	34	50.19	1350.05	379.03	1244.37	.44	.59	651.23
AH048	31	4600	8290	34	50.19	1298.28	363.25	1192.60	.46	.61	654.19
AH049	31	3700	8564	34	50.25	1186.42	329.16	1080.74	.49	.65	660.61
AH050	31	2630	8899	34	50.27	1051.84	288.14	946.16	.70	.93	668.10

STATION	CHAINAGE (E-W) MILES FEET	CHAINAGE (W-E) METRES	LATITUDE DEG MIN	ELEVATION R.L. (FEET)	ELEVATION A.H.D. (METRES)	ELEVATION MSLPA (FEET)	TERRAIN CORRECTIONS (MGAL) 2.0	TERRAIN CORRECTIONS (MGAL) 2.67	OBSERVED GRAVITY (MGAL)
AH051	31 1548	9220	34 50.24	1091.95	300.37	986.27	.45	.60	666.18
AH052	31 946	9403	34 50.23	1092.63	300.57	986.95	.40	.53	666.17
AH053	31 291	9603	34 50.22	1068.78	293.30	963.10	.40	.53	667.09
AH054	30 4746	9855	34 50.20	1162.84	321.97	1057.16	.42	.56	660.79
AH055	30 3996	10083	34 50.18	1119.66	308.81	1013.98	.29	.39	663.36
AH056	30 3296	10297	34 50.16	1156.31	319.98	1050.63	.29	.39	660.84
AH057	30 2450	10554	34 50.12	1181.96	327.80	1076.28	.25	.33	658.97
AH058	30 1900	10722	34 50.11	1147.79	317.39	1042.11	.22	.29	660.81
AH059	30 1500	10844	34 50.10	1164.99	322.63	1059.31	.19	.25	659.42
AH060	30 1000	10996	34 50.08	1204.14	334.56	1098.46	.18	.24	656.76
AH061	30 600	11118	34 50.06	1215.28	337.96	1109.60	.19	.25	655.96
AH062	30 170	11249	34 50.03	1240.62	345.68	1134.94	.20	.27	654.19
AH063	29 5000	11387	34 50.01	1259.31	351.38	1153.63	.30	.40	652.80
AH064	29 4375	11577	34 49.98	1336.84	375.01	1231.16	.38	.51	647.55
AH065	29 3825	11745	34 49.96	1301.37	364.20	1195.69	.37	.49	650.67
AH066	29 3483	11849	34 49.95	1374.21	386.40	1268.53	.35	.47	645.51
AH067	29 3000	11996	34 49.92	1445.67	408.18	1339.99	.38	.51	641.10
AH068	29 2225	12232	34 49.86	1458.34	412.04	1352.66	.32	.43	639.99
AH069	29 780	12697	34 49.78	1348.95	378.70	1243.27	.28	.37	645.62
AH070	28 5200	12935	34 49.73	1327.37	372.12	1221.69	.35	.47	646.39
AH071	28 4600	13118	34 49.69	1278.10	357.10	1172.42	.34	.45	649.22
AH072	28 4000	13301	34 49.65	1204.33	334.62	1098.65	.35	.47	653.60
GO073	28 3150	13560	34 49.64	1117.96	308.29	1012.28	.30	.40	658.22
GA074	28 2200	13849	34 49.64	1193.46	331.31	1087.78	.34	.45	653.94
GA075	28 1605	14031	34 49.64	1272.33	355.35	1166.65	.34	.45	649.57
GA076	28 1000	14215	34 49.64	1353.17	379.99	1247.49	.30	.40	644.79
GA077	28 200	14459	34 49.64	1340.43	376.10	1234.75	.25	.33	645.88
GA078	27 4800	14666	34 49.62	1375.74	386.86	1270.06	.26	.35	643.63
GA079	27 3800	14971	34 49.63	1387.16	390.35	1281.48	.30	.40	642.62
GA080	27 3098	15185	34 49.65	1383.15	389.12	1277.47	.18	.24	642.85
GA081	27 2400	15398	34 49.69	1365.58	383.77	1259.90	.20	.27	643.68
GA082	27 1700	15611	34 49.75	1344.41	377.32	1238.73	.20	.27	644.75
GA083	27 1000	15824	34 49.80	1367.10	384.23	1261.42	.22	.29	643.42
GA084	27 400	16007	34 49.86	1396.20	393.10	1290.52	.22	.29	641.80
GA085	26 5000	16215	34 49.87	1342.28	376.67	1236.60	.26	.35	644.54
GA086	26 4218	16453	34 49.87	1321.81	370.43	1216.13	.19	.25	646.08
GA087	26 3418	16697	34 49.84	1342.44	376.71	1236.76	.23	.31	645.66
GA088	26 2993	16826	34 49.83	1292.68	361.55	1187.00	.20	.27	648.10
GA089	26 400	17617	34 49.85	1329.71	372.83	1224.03	.14	.19	647.14
GA090	25 5200	17763	34 49.86	1359.61	381.95	1253.93	.13	.17	645.62
GA091	25 4600	17946	34 49.88	1379.64	388.05	1273.96	.13	.17	644.89
GA092	25 4200	18068	34 49.88	1397.15	393.39	1291.47	.13	.17	643.96
GA093	25 3600	18251	34 49.89	1420.35	400.46	1314.67	.16	.21	642.67
GA094	25 3000	18433	34 49.89	1438.15	405.89	1332.47	.12	.16	641.83
GA095	25 2400	18616	34 49.90	1424.39	401.69	1318.71	.12	.16	642.68
GA096	25 1598	18861	34 49.90	1466.48	414.52	1360.80	.11	.15	639.56
GA097	25 1100	19013	34 49.91	1504.93	426.24	1399.25	.14	.19	637.81
GA098	25 600	19165	34 49.91	1469.69	415.50	1364.01	.17	.23	639.97
GA099	25 25	19340	34 49.92	1473.17	416.56	1367.49	.13	.17	639.53
GA100	24 5000	19433	34 49.92	1498.81	424.38	1393.11	.16	.21	637.23

STATION	CHAINAGE			LATITUDE		ELEVATION			TERRAIN CORRECTIONS (MGAL)		OBSERVED GRAVITY
	(E-W)		(W-E)			R.L.	A.H.D.	MSLPA			
	MILES	FEET	METRES	DEG	MIN	(FEET)	(METRES)	(FEET)	2.0	2.67	(MGAL)
GA101	24	4200	19677	34	49.90	1446.92	408.56	1341.24	.15	.20	640.49
GA102	24	3400	19921	34	49.86	1363.62	383.17	1257.94	.16	.21	645.46
GA103	24	2700	20134	34	49.84	1330.13	372.96	1224.45	.13	.17	647.48
GA104	24	1725	20431	34	49.82	1386.67	390.20	1280.99	.15	.20	644.41
GA105	24	1200	20591	34	49.80	1362.13	382.72	1256.45	.18	.24	645.68
GA106	24	600	20774	34	49.79	1309.51	366.68	1203.83	.14	.19	648.77
GA107	24	25	20950	34	49.76	1321.22	370.25	1215.54	.16	.21	648.00
GA108	23	4800	21104	34	49.74	1347.56	378.28	1241.88	.15	.20	645.24
GA109	23	3800	21407	34	49.70	1314.32	368.14	1208.64	.16	.21	647.12
GA110	23	2900	21683	34	49.65	1305.00	365.30	1199.32	.12	.16	648.17
GA111	23	2000	21957	34	49.62	1343.52	377.04	1237.84	.14	.19	646.32
GA112	23	1400	22140	34	49.62	1307.92	366.19	1202.24	.12	.16	648.57
GA113	23	800	22323	34	49.62	1340.91	376.25	1235.23	.16	.21	646.25
GA114	23	400	22445	34	49.61	1357.05	381.17	1251.37	.11	.15	645.26
GA115	22	5000	22652	34	49.60	1334.07	374.16	1228.39	.09	.12	645.87
GA116	22	4400	22835	34	49.59	1346.34	377.90	1240.66	.10	.13	644.37
GA117	22	3800	23018	34	49.56	1366.10	383.93	1260.42	.08	.11	642.78
GA118	22	2875	23300	34	49.54	1465.23	414.14	1359.55	.07	.09	636.92
GA119	22	2400	23444	34	49.52	1454.36	410.83	1348.68	.06	.08	637.23
GA120	22	1700	23658	34	49.50	1422.48	401.11	1316.80	.04	.05	638.87
GA121	22	1200	23810	34	49.49	1408.65	396.90	1302.97	.04	.05	639.45
GA122	22	600	23993	34	49.48	1408.39	396.82	1302.71	.04	.05	639.24
BC123	21	5120	24225	34	49.43	1386.21	390.06	1280.53	.03	.04	640.80
BW124	21	4600	24383	34	49.44	1386.98	390.29	1281.30	.05	.07	640.28
BW125	21	4100	24536	34	49.40	1394.09	392.46	1288.41	.04	.05	639.95
BW126	21	3600	24688	34	49.38	1387.07	390.32	1281.39	.04	.05	640.45
BW127	21	3200	24810	34	49.34	1372.67	385.93	1266.99	.04	.05	641.73
BW128	21	2600	24993	34	49.30	1366.63	384.09	1260.95	.06	.08	641.33
BW129	21	2000	25176	34	49.24	1375.24	386.71	1269.56	.05	.07	640.65
BW130	21	1400	25359	34	49.21	1392.33	391.92	1286.65	.05	.07	639.59
BW131	21	800	25541	34	49.17	1398.92	393.93	1293.24	.06	.08	638.74
BW132	21	200	25724	34	49.12	1427.40	402.61	1321.72	.07	.09	636.66
BW133	20	5000	25871	34	49.10	1434.09	404.65	1328.41	.06	.08	636.35
BW134	20	4600	25993	34	49.06	1419.51	400.21	1313.83	.07	.09	636.81
BW135	20	4000	26175	34	49.02	1408.59	396.88	1302.91	.06	.08	636.97
BW136	20	3400	26358	34	48.98	1428.98	403.09	1323.30	.07	.09	635.90
BW137	20	2800	26541	34	48.95	1447.32	408.68	1341.64	.08	.11	634.51
BW138	20	2275	26701	34	48.91	1480.90	418.92	1375.22	.06	.08	632.09
BW139	20	1800	26846	34	48.88	1455.57	411.20	1349.89	.06	.08	633.65
BW140	20	1200	27029	34	48.83	1469.17	415.34	1363.49	.06	.08	632.38
BW141	20	600	27212	34	48.79	1453.51	410.57	1347.83	.09	.12	633.34
BW142	20	0	27395	34	48.76	1487.39	420.90	1381.71	.10	.13	630.85
BW143	19	4600	27602	34	48.70	1474.72	417.03	1369.04	.06	.08	631.35
BW144	19	4400	27663	34	48.68	1463.29	413.55	1357.61	.07	.09	631.90
BW145	19	3800	27846	34	48.64	1505.44	426.40	1399.76	.07	.09	629.36
BW146	19	3400	27968	34	48.62	1550.80	440.22	1445.12	.07	.09	626.51
BW147	19	2800	28151	34	48.57	1505.22	426.33	1399.54	.08	.11	629.18
BW148	19	2400	28272	34	48.53	1473.17	416.56	1367.49	.06	.08	631.05
BW149	19	1600	28516	34	48.49	1471.35	416.01	1365.67	.06	.08	631.03
BW150	19	990	28700	34	48.48	1480.03	418.45	1374.35	.06	.08	630.93

STATION	CHAINAGE (E-W) MILES	FEET	CHAINAGE (W-E) METRES	LATITUDE DEG	MIN	ELEVATION R.L. (FEET)	A.H.D. (METRES)	MSLPA (FEET)	TERRAIN CORRECTIONS (MGAL) 2.0	2.67	OBSERVED GRAVITY (MGAL)
BW151	19	400	28882	34	48.45	1497.92	424.11	1392.24	.05	.07	629.09
BW152	18	5200	29028	34	48.45	1515.71	429.53	1410.03	.04	.05	628.01
BW153	18	4600	29211	34	48.45	1541.97	437.53	1436.29	.05	.07	626.06
BW154	18	4000	29394	34	48.45	1552.51	440.74	1446.83	.04	.05	625.22
BW155	18	3400	29577	34	48.46	1530.25	433.96	1424.57	.03	.04	626.83
BW156	18	2800	29760	34	48.48	1520.85	431.09	1415.17	.03	.04	627.38
BW157	18	2200	29943	34	48.48	1518.02	430.23	1412.34	.02	.03	627.77
BW158	18	1800	30065	34	48.49	1519.04	430.54	1413.36	.02	.03	627.60
BW159	18	1400	30187	34	48.49	1527.22	433.04	1421.54	.01	.01	627.12
BW160	18	800	30369	34	48.50	1545.82	438.70	1440.14	.01	.01	625.88
BW161	18	200	30552	34	48.51	1564.93	444.53	1459.25	.02	.03	624.62
BW162	17	4800	30760	34	48.52	1578.34	448.62	1472.66	.02	.03	623.62
BW163	17	4200	30942	34	48.53	1563.19	444.00	1457.51	.02	.03	624.57
BW164	17	3600	31125	34	48.54	1551.86	440.55	1446.18	.02	.03	625.34
BW165	17	3000	31308	34	48.55	1543.74	438.07	1438.06	.03	.04	625.96
BW166	17	2730	31391	34	48.54	1535.18	435.46	1429.50	.04	.05	626.53
BW167	17	2600	31430	34	48.56	1538.12	436.36	1432.44	.04	.05	626.35
BW168	17	2000	31613	34	48.58	1552.04	440.60	1446.36	.07	.09	625.54
BW169	17	1400	31796	34	48.59	1566.06	444.87	1460.38	.08	.11	624.46
BW170	17	440	32089	34	48.68	1620.00	461.31	1514.32	.10	.13	621.66
BW171	16	4595	32431	34	48.72	1567.25	445.24	1461.57	.13	.17	625.78
BW172	16	4100	32582	34	48.71	1560.03	443.04	1454.35	.18	.24	626.38
BW173	16	3600	32735	34	48.69	1517.28	430.01	1411.60	.14	.19	628.84
BW174	16	3200	32857	34	48.71	1506.89	426.84	1401.21	.12	.16	629.34
BW175	16	2600	33040	34	48.77	1507.34	426.98	1401.66	.14	.19	630.06
BW176	16	2200	33161	34	48.81	1482.53	419.41	1376.85	.20	.27	631.79
TK177	16	1932	33243	34	48.82	1422.32	401.06	1316.64	.12	.16	635.77
TK178	16	1600	33344	34	48.90	1425.70	402.09	1320.02	.09	.12	635.97
TK179	16	1000	33527	34	48.96	1470.08	415.62	1364.40	.09	.12	633.63
TK180	16	400	33710	34	49.00	1442.33	407.16	1336.65	.10	.13	635.66
TK181	15	5200	33856	34	49.05	1432.55	404.18	1326.87	.08	.11	636.60
TK182	15	4600	34039	34	49.13	1469.73	415.51	1364.05	.10	.13	634.62
TK183	15	4000	34222	34	49.19	1488.43	421.21	1382.75	.13	.17	633.69
TK184	15	3400	34405	34	49.24	1479.88	418.61	1374.20	.13	.17	634.44
TK185	15	2800	34588	34	49.32	1478.51	418.19	1372.83	.11	.15	634.76
TK186	15	2200	34771	34	49.39	1447.35	408.69	1341.67	.16	.21	636.85
TK187	15	1600	34954	34	49.44	1389.21	390.97	1283.53	.12	.16	640.56
TK188	15	800	35197	34	49.54	1391.02	391.52	1285.34	.12	.16	640.70
TK189	15	200	35380	34	49.60	1422.53	401.13	1316.85	.12	.16	638.92
TK190	14	4950	35542	34	49.64	1422.54	401.13	1316.86	.12	.16	638.97
TK191	14	4400	35710	34	49.69	1394.47	392.57	1288.79	.14	.19	640.90
TK192	14	3800	35892	34	49.73	1359.60	381.95	1253.92	.15	.20	643.20
TK193	14	3200	36075	34	49.79	1300.72	364.00	1195.04	.13	.17	646.92
TK194	14	2800	36197	34	49.82	1277.03	356.78	1171.35	.11	.15	648.53
TK195	14	2475	36296	34	49.83	1277.57	356.94	1171.89	.09	.12	648.75
TK196	14	2000	36441	34	49.88	1299.70	363.69	1194.02	.16	.21	647.52
TK197	14	1400	36624	34	49.91	1353.56	380.10	1247.88	.13	.17	644.58
TK198	14	800	36807	34	49.95	1337.58	375.23	1231.90	.13	.17	645.77
TK199	14	200	36990	34	50.02	1306.76	365.84	1201.08	.13	.17	647.89
TK200	13	4800	37197	34	50.09	1272.49	355.39	1166.81	.15	.20	650.19

STATION	CHAINAGE			LATITUDE		ELEVATION			TERRAIN CORRECTIONS (MGAL)		OBSERVED GRAVITY
	(E-W)		(W-E)			R.L.	A.H.D.	MSLPA			GRAVITY
	MILES	FEET	METRES	DEG	MIN	(FEET)	(METRES)	(FEET)	2.0	2.67	(MGAL)
TK201	13	4200	37380	34	50.13	1222.38	340.12	1116.70	.18	.24	653.34
TK202	13	3600	37563	34	50.18	1200.40	333.42	1094.72	.19	.25	655.00
TK203	13	3000	37746	34	50.22	1162.00	321.72	1056.32	.11	.15	657.41
TK204	13	2400	37929	34	50.28	1156.48	320.03	1050.80	.10	.13	658.19
TK205	13	1800	38111	34	50.33	1165.84	322.89	1060.16	.10	.13	658.08
TK206	13	1400	38233	34	50.36	1134.22	313.25	1028.54	.13	.17	660.12
TK207	13	800	38416	34	50.41	1122.12	309.56	1016.44	.11	.15	661.09
TK208	13	200	38599	34	50.45	1143.46	316.07	1037.78	.10	.13	659.93
TK209	12	4800	38806	34	50.51	1130.08	311.99	1024.40	.08	.11	660.83
TK210	12	4200	38989	34	50.56	1160.89	321.38	1055.21	.10	.13	659.05
TK211	12	3600	39172	34	50.60	1186.46	329.17	1080.78	.11	.15	657.65
TK212	12	3000	39355	34	50.65	1207.27	335.51	1101.59	.13	.17	656.55
TK213	12	2400	39538	34	50.69	1269.49	354.48	1163.81	.12	.16	652.91
TK214	12	1800	39721	34	50.74	1293.10	361.68	1187.42	.12	.16	651.40
TK215	12	1200	39904	34	50.78	1294.67	362.15	1188.99	.13	.17	651.30
TK216	12	600	40086	34	50.82	1295.92	362.54	1190.24	.18	.24	651.17
TK217	12	0	40269	34	50.86	1279.92	357.66	1174.24	.19	.25	652.00
TK218	11	4800	40416	34	50.90	1279.92	357.66	1174.24	.24	.32	652.87
TK219	11	4200	40599	34	50.93	1266.09	353.44	1160.41	.24	.32	654.36
TK220	11	3600	40781	34	50.98	1241.67	346.00	1135.99	.28	.37	655.47
TK221	11	3283	40879	34	51.03	1222.11	340.04	1116.43	.27	.36	656.20
TK222	11	3000	40964	34	51.03	1209.29	336.13	1103.61	.29	.39	656.09
TK223	11	2400	41147	34	51.06	1196.59	332.26	1090.91	.31	.41	656.71
TK224	11	1810	41327	34	51.10	1177.15	326.33	1071.47	.35	.47	657.64
TK225	11	1400	41452	34	51.11	1127.68	311.26	1022.00	.36	.48	660.38
TK226	11	1270	41492	34	51.14	1113.36	306.89	1007.68	.33	.44	661.19
TK228	10	5200	41903	34	51.22	879.43	235.59	773.75	.47	.63	673.92
TK229	10	4600	42086	34	51.24	933.51	252.07	827.83	.40	.53	670.82
TK230	10	4000	42269	34	51.28	956.86	259.19	851.18	.42	.56	669.18
TK231	10	3400	42452	34	51.31	924.04	249.04	818.36	.36	.48	672.62
TK232	10	2800	42635	34	51.35	853.23	227.60	747.55	.35	.47	675.39
TK233	10	2200	42817	34	51.38	893.17	239.78	787.49	.34	.45	673.16
TK234	10	1600	43000	34	51.40	935.02	252.53	829.34	.32	.43	670.60
TK235	10	1225	43115	34	51.40	961.44	260.59	855.76	.36	.48	668.90
TK236	10	625	43298	34	51.43	902.19	242.53	796.51	.34	.45	672.70
TK237	10	225	43419	34	51.44	860.78	229.90	755.10	.31	.41	675.20
TK238	9	4975	43581	34	51.45	845.44	225.23	739.76	.35	.47	676.40
TK239	9	4375	43764	34	51.48	793.86	209.51	688.18	.39	.52	678.39
TK240	9	3800	43939	34	51.49	729.72	189.96	624.04	.27	.36	682.17
TK241	9	3200	44122	34	51.51	699.87	180.86	594.19	.25	.33	684.34
TK242	9	2800	44244	34	51.52	679.88	174.77	574.20	.24	.32	685.48
TK243	9	2400	44366	34	51.53	665.51	170.39	559.83	.21	.28	686.64
TK244	9	2000	44488	34	51.54	659.63	168.59	553.95	.20	.27	687.34
TK245	9	1400	44671	34	51.55	639.04	162.32	533.36	.18	.24	689.00
TK246	9	400	44975	34	51.54	601.85	150.98	496.17	.16	.21	691.59
TK247	9	0	45097	34	51.55	583.93	145.52	478.25	.16	.21	692.77
TK248	8	4800	45244	34	51.57	573.81	142.44	468.13	.11	.15	693.81
TK249	8	4200	45427	34	51.61	566.00	140.06	460.32	.09	.12	694.57
TK250	8	3400	45670	34	51.65	569.70	141.18	464.02	.07	.09	694.83
F0251	8	3216	45727	34	51.67	569.96	141.26	464.28	.06	.08	694.85

STATION	CHAINAGE (E-W) MILES	FEET	(W-E) METRES	LATITUDE DEG	MIN	ELEVATION R.L. (FEET)	A.H.D. (METRES)	MSLPA (FEET)	TERRAIN CORRECTIONS (MGAL) 2.0	2.67	OBSERVED GRAVITY (MGAL)
PM252	8	2800	45853	34	51.70	566.06	140.07	460.38	.05	.07	695.20
PM253	8	2200	46036	34	51.74	575.29	142.89	469.61	.04	.05	694.35
PM254	8	1600	46219	34	51.77	588.65	146.96	482.97	.04	.05	693.81
PM255	8	1000	46402	34	51.82	605.42	152.07	499.74	.03	.04	692.35
PM256	8	400	46585	34	51.86	618.74	156.13	513.06	.03	.04	691.34
PM257	8	240	46634	34	51.87	620.57	156.69	514.89	.04	.05	691.28
PM258	7	5200	46731	34	51.89	617.97	155.90	512.29	.02	.03	691.61
PM259	7	4600	46914	34	51.92	610.23	153.54	504.55	.02	.03	692.22
PM260	7	4000	47097	34	51.96	602.17	151.08	496.49	.02	.03	693.08
PM261	7	3400	47280	34	52.00	594.42	148.72	488.74	.02	.03	693.16
PM262	7	2000	47706	34	52.10	570.45	141.41	464.77	.03	.04	695.22
PM263	7	800	48072	34	52.20	565.35	139.86	459.67	.03	.04	695.90
PM264	7	200	48255	34	52.25	570.41	141.40	464.73	.03	.04	695.61
PM265	6	5040	48389	34	52.31	574.00	142.49	468.32	.03	.04	695.76
PM266	6	5000	48401	34	52.29	578.48	143.86	472.80	.03	.04	695.65
PM267	6	4400	48584	34	52.34	581.16	144.68	475.48	.03	.04	695.82
PM268	6	3800	48767	34	52.39	582.81	145.18	477.13	.03	.04	695.39
PM269	6	3200	48950	34	52.44	594.19	148.65	488.51	.03	.04	695.00
PM270	6	2600	49133	34	52.50	599.78	150.35	494.10	.03	.04	694.65
PM271	6	2100	49285	34	52.54	584.64	145.74	478.96	.03	.04	695.35
PM272	6	1400	49499	34	52.60	578.80	143.96	473.12	.03	.04	696.08
PM273	6	800	49682	34	52.64	577.64	143.60	471.96	.03	.04	696.12
PM274	6	200	49864	34	52.69	571.85	141.84	466.17	.03	.04	696.18
PM275	5	5600	50011	34	52.73	564.33	139.55	458.65	.03	.04	696.65
PM276	5	4400	50194	34	52.77	546.23	134.03	440.55	.03	.04	697.65
PM277	5	3800	50377	34	52.84	529.23	128.85	423.55	.03	.04	699.24
PM278	5	3200	50559	34	52.88	515.83	124.76	410.15	.03	.04	700.32
PM279	5	2600	50742	34	52.92	503.66	121.05	397.98	.03	.04	700.83
PM280	5	2000	50925	34	52.98	487.87	116.24	382.19	.03	.04	701.63
PM281	5	1695	51018	34	53.04	487.92	116.26	382.24	.04	.05	701.75
PM282	5	1000	51230	34	53.06	471.13	111.14	365.45	.03	.04	702.89
PM283	5	400	51413	34	53.11	454.82	106.17	349.14	.03	.04	704.57
PM284	4	5000	51620	34	53.18	446.46	103.62	340.78	.03	.04	705.37
PM285	4	4199	51864	34	53.26	440.90	101.93	335.22	.03	.04	705.96
PM286	4	3395	52109	34	53.31	432.20	99.27	326.52	.03	.04	706.97
MN287	4	2600	52352	34	53.38	428.83	98.25	323.15	.03	.04	707.25
MN288	4	1800	52595	34	53.44	414.16	93.77	308.48	.03	.04	708.38
MN289	4	1200	52778	34	53.50	409.94	92.49	304.26	.03	.04	708.87
MN290	4	600	52961	34	53.55	403.96	90.67	298.28	.03	.04	709.24
MN291	3	5200	53169	34	53.58	396.40	88.36	290.72	.03	.04	709.75
MN292	3	4600	53351	34	53.60	388.84	86.06	283.16	.03	.04	710.11
MN293	3	4000	53534	34	53.62	379.90	83.33	274.22	.03	.04	711.10
MN294	3	3400	53717	34	53.65	376.27	82.23	270.59	.03	.04	711.18
MN295	3	2600	53961	34	53.71	377.02	82.45	271.34	.04	.05	711.39
MN296	3	2000	54144	34	53.76	374.28	81.62	268.60	.05	.07	711.42
MN297	3	1375	54334	34	53.83	360.00	77.27	254.32	.04	.05	711.83
MN298	3	600	54571	34	53.87	350.59	74.40	244.91	.03	.04	711.27
MN299	3	0	54753	34	53.90	340.85	71.43	235.17	.03	.04	710.62
MN300	2	4500	54900	34	53.93	333.77	69.27	228.09	.03	.04	709.68
MN301	2	4200	55083	34	53.96	325.23	66.67	219.55	.03	.04	709.67

STATION	CHAINAGE			LATITUDE		ELEVATION			TERRAIN CORRECTIONS (MGAL)		OBSERVED GRAVITY
	(E-W)		(W-E)			R.L.	A.H.D.	MSLPA			
	MILES	FEET	METRES	DEG	MIN	(FEET)	(METRES)	(FEET)	2.0	2.67	(MGAL)
MN332	2	3700	55235	34	54.03	319.84	65.03	214.16	.03	.04	709.85
MN303	2	2600	55570	34	54.08	314.63	63.44	208.95	.03	.04	710.16
PN304	2	2000	55753	34	54.12	324.38	66.41	218.70	.03	.04	709.55
SN305	2	1400	55936	34	54.17	326.88	67.17	221.20	.03	.04	709.38
MN306	2	800	56119	34	54.22	328.26	67.59	222.58	.03	.04	709.20
MN307	2	193	56304	34	54.27	335.65	69.85	229.97	.03	.04	708.67
MN308	1	4019	56747	34	54.38	344.19	72.45	238.51	.03	.04	708.14
MN309	1	3400	56936	34	54.43	340.43	71.30	234.75	.03	.04	708.48
MN310	1	2801	57118	34	54.48	346.95	73.29	241.27	.03	.04	708.17
MN312	1	400	57850	34	54.71	285.37	54.52	179.69	.03	.04	713.03
MN313	0	4800	58118	34	54.84	273.38	50.87	167.70	.03	.04	714.03
MN314	0	3820	58415	34	54.96	262.22	47.46	156.54	.04	.05	715.20
MN315	0	3524	58507	34	54.98	248.50	43.28	142.82	.04	.05	716.18

STATION	THEORETICAL GRAVITY (MGAL) 979000+	FREE-AIR ANOMALY (MGAL)	REGIONAL ELEVATION (METRES)	REGIONAL FREE-AIR ANOMALY (MGAL)	BOUGUER ANOMALIES AT 2.67 (MGAL)		
					RAW	REGIONAL	RESIDUAL
AH001	732.28	9.81	202.83	11.62	-9.70	-10.06	.36
AH002	732.16	11.53	238.13	16.06	-10.74	-9.80	-.95
AH003	732.03	12.36	254.23	18.09	-11.91	-9.68	-2.23
AH004	731.93	13.15	263.60	19.26	-11.21	-9.61	-1.60
AH005	731.93	13.04	266.92	19.68	-10.92	-9.58	-1.33
AH006	731.96	12.73	270.48	20.13	-11.14	-9.56	-1.58
AH007	731.99	15.51	279.51	21.27	-10.74	-9.49	-1.25
AH008	732.04	19.90	285.64	22.03	-9.40	-9.44	.04
AH009	732.06	24.21	291.24	22.71	-8.58	-9.40	.82
AH010	732.10	26.66	294.13	23.06	-8.04	-9.38	1.34
AH011	732.19	28.42	303.43	24.23	-7.43	-9.31	1.88
AH012	732.20	29.18	308.69	24.85	-7.00	-9.23	2.22
AH013	732.23	30.04	311.66	25.19	-7.05	-9.17	2.12
AH014	732.21	33.21	318.31	25.97	-7.07	-9.04	1.97
AH015	732.20	33.42	323.92	26.62	-8.00	-8.93	.93
AH016	732.20	30.93	329.91	27.35	-7.97	-8.79	.83
AH017	732.20	31.33	333.08	27.75	-8.16	-8.71	.56
AH018	732.20	32.13	337.44	28.31	-8.10	-8.60	.50
AH019	732.20	33.24	341.35	28.83	-8.31	-8.49	.19
AH020	732.10	35.06	351.70	30.25	-10.22	-8.17	-2.04
AH021	732.03	32.01	365.37	32.11	-10.36	-7.68	-2.68
AH022	732.02	31.75	367.71	32.44	-10.29	-7.59	-2.70
AH023	732.00	31.64	372.27	33.07	-9.95	-7.40	-2.55
AH024	732.00	32.42	375.09	33.47	-9.84	-7.28	-2.55
AH025	732.00	32.56	377.02	33.78	-9.52	-7.19	-2.33
AH026	732.00	32.95	379.87	34.41	-8.72	-7.02	-1.70
AH027	731.99	33.84	381.65	35.00	-7.51	-6.86	-.65
AH028	731.99	34.73	382.59	35.33	-7.03	-6.76	-.28
AH029	731.99	35.20	383.25	35.51	-7.21	-6.69	-.51
AH030	732.00	38.10	385.04	36.42	-5.25	-6.37	1.13
AH031	732.00	38.07	385.21	36.67	-4.78	-6.29	1.51
AH032	732.00	38.43	385.14	36.77	-4.61	-6.25	1.63
AH033	731.99	39.15	384.21	37.16	-4.23	-6.07	1.84
AH034	731.97	39.49	384.22	37.17	-4.12	-5.95	1.83
AH035	731.97	38.98	384.65	37.12	-4.12	-5.84	1.73
AH036	731.96	38.71	384.76	36.99	-3.89	-5.73	1.84
AH037	731.95	39.70	384.18	36.81	-4.25	-5.57	1.31
AH038	731.96	39.70	383.73	36.74	-4.20	-5.51	1.32
AH039	731.96	37.50	381.76	36.50	-4.13	-5.35	1.23
AH040	731.95	38.35	376.97	36.23	-4.50	-5.18	.68
AH041	731.92	35.86	370.88	35.89	-4.40	-5.10	.70
AH042	731.95	36.37	366.87	35.53	-4.71	-5.09	.38
AH043	731.95	37.17	363.50	35.24	-4.66	-5.11	.44
AH044	731.95	38.22	359.51	34.87	-5.17	-5.16	-.00
AH045	731.90	38.98	356.23	34.48	-4.81	-5.25	.44
AH046	731.72	39.85	355.34	34.37	-5.18	-5.28	.10
AH047	731.72	36.47	348.79	33.62	-5.32	-5.51	.20
AH048	731.72	34.56	346.91	33.34	-5.44	-5.61	.17
AH049	731.81	30.37	342.67	32.72	-5.77	-5.86	.09
AH050	731.83	25.18	338.23	32.05	-6.10	-6.18	.08

STATION	THEORETICAL GRAVITY (MGAL) 979000+	FREE-AIR ANOMALY (MGAL)	REGIONAL ELEVATION (METRES)	REGIONAL FREE-AIR ANOMALY (MGAL)	BOUGUER ANOMALIES AT 2.67 (MGAL)		
					RAW	REGIONAL	RESIDUAL
AH051	731.79	27.07	336.07	31.64	-5.91	-6.52	.61
AH052	731.78	27.14	335.41	31.43	-5.93	-6.70	.77
AH053	731.76	25.83	335.36	31.43	-6.42	-6.90	.47
AH054	731.74	28.41	334.55	31.43	-7.03	-7.15	.13
AH055	731.71	26.94	335.01	31.25	-7.19	-7.40	.21
AH056	731.68	27.90	336.06	30.91	-7.49	-7.63	.14
AH057	731.62	28.50	337.97	30.44	-7.81	-7.93	.11
AH058	731.61	27.14	339.76	30.15	-8.05	-8.12	.07
AH059	731.59	27.38	341.51	29.93	-8.43	-8.26	-.18
AH060	731.57	28.43	344.01	29.67	-8.73	-8.43	-.30
AH061	731.54	28.71	345.91	29.47	-8.82	-8.58	-.25
AH062	731.50	29.36	347.50	29.29	-9.02	-8.73	-.29
AH063	731.47	29.76	348.06	29.24	-9.12	-8.87	-.25
AH064	731.42	31.84	348.30	29.33	-9.57	-9.06	-.51
AH065	731.40	30.95	349.48	29.45	-9.27	-9.23	-.04
AH066	731.38	33.36	350.26	29.52	-9.37	-9.34	-.03
AH067	731.34	35.71	351.46	29.63	-9.41	-9.48	.07
AH068	731.26	35.88	355.13	29.89	-9.76	-9.68	-.08
AH069	731.14	31.33	361.91	30.30	-10.63	-10.05	-.58
AH070	731.07	30.14	365.74	30.47	-10.99	-10.24	-.75
AH071	731.02	28.39	368.42	30.53	-11.07	-10.39	-.69
AH072	730.96	25.89	370.45	30.64	-11.05	-10.53	-.52
GA073	730.95	22.40	372.38	30.82	-11.66	-10.69	-.97
GA074	730.95	25.23	373.12	30.86	-11.36	-10.88	-.48
GA075	730.95	28.27	373.65	30.82	-11.00	-10.98	-.02
GA076	730.95	31.10	372.10	30.73	-10.98	-11.06	.08
GA077	730.95	30.99	369.84	30.50	-10.72	-11.18	.46
GA078	730.92	32.09	368.67	30.19	-10.81	-11.26	.44
GA079	730.93	32.14	367.34	29.81	-11.10	-11.32	.22
GA080	730.96	31.96	366.85	29.73	-11.30	-11.33	.03
GA081	731.02	31.08	367.62	29.79	-11.55	-11.31	-.24
GA082	731.10	30.08	370.18	29.95	-11.84	-11.26	-.58
GA083	731.17	30.81	374.00	30.27	-11.85	-11.19	-.65
GA084	731.26	31.84	376.84	30.68	-11.81	-11.13	-.68
GA085	731.27	29.50	379.08	31.21	-12.26	-11.04	-1.23
GA086	731.27	29.11	380.58	31.74	-12.05	-10.97	-1.08
GA087	731.23	30.14	382.04	32.13	-11.66	-10.89	-.77
GA088	731.21	28.45	382.91	32.28	-11.70	-10.85	-.85
GA089	731.24	30.94	388.86	32.67	-10.55	-10.74	.19
GA090	731.26	32.22	389.53	32.65	-10.30	-10.71	.41
GA091	731.28	33.35	389.47	32.72	-9.86	-10.65	.79
GA092	731.28	34.06	388.99	32.79	-9.74	-10.61	.86
GA093	731.30	34.94	388.60	32.86	-9.61	-10.54	.92
GA094	731.30	35.78	389.16	32.84	-9.44	-10.47	1.03
GA095	731.31	35.32	389.61	32.82	-9.43	-10.42	.99
GA096	731.31	36.16	389.27	32.85	-10.04	-10.38	.34
GA097	731.33	38.01	389.68	32.87	-9.45	-10.35	.90
GA098	731.33	36.85	390.33	32.86	-9.37	-10.32	.95
GA099	731.34	36.73	390.78	32.91	-9.67	-10.28	.62
GA100	731.34	36.83	390.88	33.96	-10.40	-10.22	

STATION	THEORETICAL GRAVITY (MGAL) 979000+	FREE-AIR ANOMALY (MGAL)	REGIONAL ELEVATION (METRES)	REGIONAL FREE-AIR ANOMALY (MGAL)	BOUGUER ANOMALIES AT 2.67 (MGAL)		
					RAW	REGIONAL	RESIDUAL
GA101	731.31	35.25	390.91	33.10	-10.23	-10.20	-.03
GA102	731.26	32.44	390.68	33.20	-10.18	-10.16	-.02
GA103	731.23	31.34	389.78	33.25	-10.18	-10.17	-.02
GA104	731.20	33.61	388.36	33.11	-9.81	-10.26	.45
GA105	731.17	32.60	387.17	33.00	-9.94	-10.34	.40
GA106	731.16	30.76	386.11	32.94	-10.05	-10.44	.39
GA107	731.12	31.13	384.98	32.86	-10.05	-10.54	.50
GA108	731.09	30.88	384.09	32.78	-11.21	-10.65	-.57
GA109	731.03	29.69	383.57	32.52	-11.26	-10.84	-.41
GA110	730.96	29.93	382.33	32.13	-10.75	-11.05	.31
GA111	730.92	31.75	381.77	31.77	-10.22	-11.24	1.03
GA112	730.92	30.65	382.30	31.54	-10.13	-11.36	1.23
GA113	730.92	31.43	383.00	31.37	-10.42	-11.47	1.05
GA114	730.90	31.97	383.30	31.29	-10.49	-11.55	1.05
GA115	730.89	30.44	383.37	31.19	-11.27	-11.68	.41
GA116	730.88	30.10	383.63	31.11	-12.01	-11.81	-.20
GA117	730.83	30.41	384.44	30.98	-12.40	-11.95	-.44
GA118	730.81	33.91	385.42	30.89	-12.30	-12.19	-.11
GA119	730.78	33.22	386.05	30.89	-12.63	-12.31	-.32
GA120	730.75	31.89	387.68	30.84	-12.90	-12.48	-.42
GA121	730.74	31.18	389.10	30.80	-13.13	-12.59	-.55
GA122	730.72	30.97	390.43	30.82	-13.34	-12.71	-.63
PO123	730.65	30.51	391.71	30.87	-13.06	-12.91	-.15
PW124	730.67	30.05	393.06	30.87	-13.52	-13.06	-.46
PW125	730.61	30.44	394.20	30.84	-13.38	-13.22	-.16
RW126	730.58	30.31	395.53	30.82	-13.27	-13.38	.11
PW127	730.52	29.80	396.64	30.80	-13.29	-13.51	.22
BW128	730.47	29.38	398.30	30.77	-13.48	-13.71	.24
PW129	730.38	29.60	399.54	30.75	-13.57	-13.90	.33
PW130	730.34	30.18	400.27	30.78	-13.56	-14.06	.50
PW131	730.28	30.01	400.51	30.86	-13.95	-14.21	.26
BW132	730.21	30.68	401.03	30.83	-14.24	-14.35	.12
PW133	730.19	31.03	402.14	30.74	-14.13	-14.47	.34
BW134	730.13	30.17	403.39	30.65	-14.47	-14.56	.08
PW135	730.07	29.36	404.51	30.57	-14.93	-14.69	-.24
BW136	730.02	30.26	405.53	30.53	-14.70	-14.82	.11
PW137	729.97	30.64	406.66	30.53	-14.94	-14.94	-.00
BW138	729.92	31.44	407.71	30.56	-15.31	-15.06	-.26
BW139	729.88	30.66	408.80	30.60	-15.23	-15.17	-.06
BW140	729.81	30.74	410.80	30.67	-15.62	-15.31	-.31
PW141	729.75	30.28	413.11	30.70	-15.50	-15.44	-.06
BW142	729.71	31.02	415.43	30.75	-15.90	-15.58	-.32
BW143	729.62	30.41	417.46	30.82	-16.13	-15.72	-.41
PW144	729.59	29.91	418.00	30.84	-16.22	-15.76	-.46
RW145	729.54	31.39	419.40	30.90	-16.18	-15.89	-.29
BW146	729.51	32.84	420.10	30.95	-16.28	-15.98	-.30
PW147	729.44	31.29	421.45	31.03	-16.26	-16.10	-.17
BW148	729.38	30.21	422.63	31.08	-16.28	-16.17	-.11
RW149	729.33	30.07	425.07	31.16	-16.36	-16.33	-.03
BW150	729.31	30.24	426.80	31.24	-16.48	-16.42	-.06

STATION	THEORETICAL GRAVITY (MGAL) 979000+	FREE-AIR ANOMALY (MGAL)	REGIONAL ELEVATION (METRES)	REGIONAL FREE-AIR ANOMALY (MGAL)	BOUGUER ANOMALIES AT 2.67 (MGAL)		
					RAW	REGIONAL	RESIDUAL
RW151	729.27	30.69	428.23	31.30	-16.66	-16.51	-.15
RW152	729.27	31.28	429.18	31.33	-16.69	-16.58	-.11
RW153	729.27	31.80	430.24	31.37	-17.05	-16.65	-.40
RW154	729.27	31.95	431.33	31.43	-17.27	-16.73	-.54
RW155	729.28	31.45	432.17	31.54	-17.02	-16.79	-.23
RW156	729.31	31.09	433.32	31.69	-17.06	-16.84	-.23
RW157	729.31	31.21	434.89	31.79	-16.86	-16.86	-.00
RW158	729.33	31.13	435.66	31.86	-16.98	-16.85	-.13
RW159	729.33	31.41	436.20	31.94	-16.98	-16.84	-.14
RW160	729.34	31.91	437.25	31.98	-17.12	-16.84	-.28
RW161	729.35	32.43	438.49	31.96	-17.23	-16.82	-.41
RW162	729.37	32.68	439.21	31.95	-17.44	-16.78	-.67
RW163	729.38	32.19	439.53	31.97	-17.42	-16.72	-.70
RW164	729.40	31.88	439.17	32.03	-17.34	-16.65	-.70
RW165	729.41	31.72	437.91	32.06	-17.21	-16.56	-.65
RW166	729.40	31.50	437.32	32.08	-17.13	-16.51	-.61
RW167	729.42	31.57	437.05	32.08	-17.16	-16.49	-.66
RW168	729.45	32.04	435.84	32.13	-17.12	-16.38	-.74
RW169	729.47	32.27	434.58	32.19	-17.36	-16.26	-1.10
RW170	729.59	34.41	433.52	32.28	-17.02	-16.03	-.99
RW171	729.65	33.52	432.45	32.37	-16.08	-15.77	-.32
RW172	729.64	33.45	431.65	32.35	-15.84	-15.65	-.19
RW173	729.61	31.92	430.41	32.33	-15.97	-15.53	-.44
RW174	729.64	31.41	428.89	32.33	-16.14	-15.42	-.72
RW175	729.72	32.09	426.33	32.32	-15.45	-15.27	-.19
RW176	729.78	31.43	424.82	32.30	-15.19	-15.16	-.03
TK177	729.79	29.73	424.01	32.28	-14.94	-15.08	.14
TK178	729.90	30.14	423.11	32.24	-14.69	-14.98	.29
TK179	729.99	31.89	421.48	32.14	-14.45	-14.80	.35
TK180	730.04	31.25	419.57	32.00	-14.13	-14.62	.49
TK181	730.12	31.20	417.49	31.88	-13.87	-14.48	.60
TK182	730.23	32.61	413.90	31.78	-13.71	-14.29	.58
TK183	730.31	33.35	409.46	31.73	-13.56	-14.09	.53
TK184	730.38	33.23	405.30	31.65	-13.40	-13.88	.48
TK185	730.50	33.31	402.39	31.49	-13.30	-13.67	.37
TK186	730.59	32.37	399.49	31.27	-13.11	-13.47	.36
TK187	730.67	30.54	396.79	31.02	-13.01	-13.28	.27
TK188	730.81	30.71	392.67	30.66	-12.90	-13.04	.13
TK189	730.89	31.81	389.55	30.41	-12.88	-12.84	-.03
TK190	730.95	31.80	386.72	30.20	-12.88	-12.68	-.21
TK191	731.02	31.02	383.25	30.00	-12.68	-12.50	-.18
TK192	731.07	29.98	379.39	29.79	-12.51	-12.32	-.19
TK193	731.16	28.08	375.60	29.56	-12.44	-12.15	-.28
TK194	731.20	27.42	372.68	29.40	-12.32	-12.05	-.27
TK195	731.21	27.68	370.04	29.28	-12.11	-11.96	-.14
TK196	731.28	28.46	366.28	29.10	-11.99	-11.85	-.14
TK197	731.33	30.54	361.83	28.87	-11.78	-11.70	-.07
TK198	731.38	30.17	357.19	28.64	-11.60	-11.56	-.04
TK199	731.48	29.30	353.50	28.45	-11.43	-11.42	-.00
TK200	731.58	28.27	350.57	28.32	-11.26	-11.27	.02

STATION	THEORETICAL GRAVITY (MGAL) 979000+	FREE-AIR ANOMALY (MGAL)	REGIONAL ELEVATION (METRES)	REGIONAL FREE-AIR ANOMALY (MGAL)	BOUGUER ANOMALIES AT 2.67 (MGAL)		
					PAW	REGIONAL	RESIDUAL
TK201	731.64	26.65	348.26	28.26	-11.13	-11.15	.02
TK202	731.71	26.18	346.31	28.26	-10.84	-11.04	.19
TK203	731.76	24.92	344.65	28.24	-10.90	-10.93	.03
TK204	731.85	25.10	343.37	28.20	-10.55	-10.81	.26
TK205	731.92	25.79	342.60	28.17	-10.17	-10.65	.49
TK206	731.96	24.82	342.42	28.15	-10.03	-10.55	.52
TK207	732.03	24.58	342.48	28.10	-9.88	-10.43	.55
TK208	732.09	25.37	342.11	28.03	-9.83	-10.35	.52
TK209	732.17	24.93	340.42	27.99	-9.84	-10.27	.43
TK210	732.24	25.98	338.65	27.86	-9.82	-10.23	.41
TK211	732.30	26.92	337.16	27.53	-9.73	-10.21	.48
TK212	732.37	27.71	335.58	27.00	-9.62	-10.22	.60
TK213	732.42	29.87	333.71	26.46	-9.60	-10.25	.65
TK214	732.50	30.51	330.34	25.98	-9.77	-10.29	.52
TK215	732.55	30.50	326.71	25.58	-9.81	-10.32	.51
TK216	732.61	30.43	323.70	25.14	-9.86	-10.38	.52
TK217	732.67	29.70	320.97	24.68	-10.03	-10.44	.41
TK218	732.72	30.51	318.77	24.37	-9.15	-10.50	1.34
TK219	732.76	30.66	315.16	24.00	-8.53	-10.58	2.05
TK220	732.83	29.40	311.76	23.66	-8.91	-10.68	1.77
TK221	732.90	28.22	310.27	23.46	-9.43	-10.73	1.30
TK222	732.90	26.90	309.12	23.25	-10.28	-10.78	.50
TK223	732.95	26.29	306.37	22.80	-10.44	-10.87	.43
TK224	733.00	25.33	302.63	22.28	-10.68	-10.99	.31
TK225	733.02	23.41	299.47	21.85	-10.91	-11.08	.18
TK226	733.06	22.83	298.42	21.71	-11.04	-11.11	.07
TK228	733.17	13.44	283.80	20.00	-12.27	-11.42	-.85
TK229	733.20	15.40	275.95	19.14	-12.24	-11.54	-.71
TK230	733.26	15.90	267.79	18.23	-12.51	-11.63	-.88
TK231	733.30	15.36	259.48	17.29	-12.01	-11.72	-.29
TK232	733.35	12.27	251.04	16.34	-12.71	-11.80	-.91
TK233	733.40	13.75	242.50	15.39	-12.60	-11.87	-.73
TK234	733.43	15.10	234.01	14.41	-12.71	-11.95	-.76
TK235	733.43	15.88	228.79	13.81	-12.77	-12.01	-.76
TK236	733.47	14.07	220.45	12.86	-12.59	-12.10	-.49
TK237	733.48	12.66	214.91	12.27	-12.63	-12.14	-.48
TK238	733.50	12.40	208.10	11.54	-12.31	-12.18	-.13
TK239	733.54	9.50	201.36	10.76	-13.40	-12.20	-1.20
TK240	733.55	7.23	196.77	10.06	-13.64	-12.23	-1.41
TK241	733.58	6.57	192.56	9.42	-13.32	-12.26	-1.06
TK242	733.60	5.81	189.69	9.13	-13.40	-12.26	-1.14
TK243	733.61	5.61	186.58	8.88	-13.16	-12.26	-.90
TK244	733.62	5.74	183.61	8.66	-12.84	-12.24	-.60
TK245	733.64	5.45	179.82	8.29	-12.46	-12.21	-.24
TK246	733.62	4.56	174.10	7.59	-12.11	-12.18	.07
TK247	733.64	4.04	171.20	7.36	-12.02	-12.15	.13
TK248	733.67	4.10	167.52	7.12	-11.68	-12.12	.44
TK249	733.72	4.06	162.86	6.76	-11.47	-12.06	.59
TK250	733.78	4.62	157.80	6.22	-11.07	-11.99	.92
P0251	733.81	4.63	156.68	6.09	-11.08	-11.97	.89

STATION	THEORETICAL GRAVITY (MGAL) 979000+	FREE-AIR ANOMALY (MGAL)	REGIONAL ELEVATION (METRES)	REGIONAL FREE-AIR ANOMALY (MGAL)	BOUGUER ANOMALIES AT 2.67 (MGAL)		
					RAW	REGIONAL	RESIDUAL
PM252	733.85	4.57	154.29	5.82	-11.02	-11.93	.91
PM253	733.90	4.54	151.66	5.55	-11.38	-11.86	.47
PM254	733.95	5.21	149.76	5.31	-11.17	-11.79	.62
PM255	734.02	5.26	148.34	5.17	-11.70	-11.69	-.02
PM256	734.07	5.44	147.24	5.12	-11.97	-11.58	-.39
PM257	734.09	5.54	146.98	5.12	-11.92	-11.55	-.37
PM258	734.12	5.60	146.50	5.10	-11.80	-11.50	-.30
PM259	734.16	5.44	145.95	5.08	-11.70	-11.41	-.29
PM260	734.22	5.48	145.80	5.06	-11.38	-11.34	-.04
PM261	734.27	4.78	145.80	5.05	-11.82	-11.28	-.54
PM262	734.41	4.44	146.08	5.02	-11.33	-11.20	-.12
PM263	734.55	4.50	145.99	4.97	-11.09	-11.15	.06
PM264	734.62	4.62	145.49	4.91	-11.15	-11.14	-.01
PM265	734.71	5.02	144.87	4.84	-10.87	-11.14	.27
PM266	734.68	5.36	144.81	4.84	-10.68	-11.14	.46
PM267	734.75	5.71	143.60	4.75	-10.42	-11.13	.71
PM268	734.82	5.37	142.02	4.61	-10.82	-11.12	.30
PM269	734.89	5.98	140.35	4.47	-10.60	-11.09	.49
PM270	734.98	6.07	138.63	4.33	-10.70	-11.02	.32
PM271	735.03	5.29	137.08	4.20	-10.96	-10.97	.00
PM272	735.12	5.38	134.89	4.03	-10.67	-10.89	.22
PM273	735.17	5.26	133.04	3.89	-10.75	-10.82	.07
PM274	735.24	4.70	131.30	3.76	-11.11	-10.74	-.37
PM275	735.30	4.41	129.91	3.66	-11.15	-10.68	-.47
PM276	735.36	3.65	128.14	3.53	-11.29	-10.61	-.68
PM277	735.46	3.54	126.27	3.41	-10.82	-10.54	-.29
PM278	735.51	3.31	124.13	3.28	-10.60	-10.47	-.13
PM279	735.57	2.62	121.86	3.13	-10.88	-10.40	-.47
PM280	735.65	1.85	119.52	2.95	-11.11	-10.35	-.76
PM281	735.74	1.89	118.24	2.85	-11.06	-10.32	-.73
PM282	735.76	1.42	115.14	2.62	-10.97	-10.26	-.70
PM283	735.84	1.49	112.38	2.42	-10.33	-10.20	-.13
PM284	735.93	1.41	109.32	2.17	-10.13	-10.14	.00
PM285	736.05	1.36	105.76	1.87	-9.99	-10.07	.08
PM286	736.12	1.48	102.27	1.51	-9.57	-10.06	.48
MN287	736.22	1.35	98.92	1.06	-9.59	-10.12	.52
MN288	736.30	1.02	95.74	.53	-9.43	-10.25	.82
MN289	736.38	1.02	93.42	.14	-9.28	-10.37	1.09
MN290	736.46	.76	91.16	-.26	-9.33	-10.50	1.16
MN291	736.50	.52	88.63	-.70	-9.32	-10.66	1.34
MN292	736.53	.14	86.49	-1.06	-9.44	-10.79	1.35
MN293	736.56	.26	84.55	-1.40	-9.02	-10.93	1.91
MN294	736.60	-.04	82.86	-1.73	-9.20	-11.06	1.87
MN295	736.68	.15	80.80	-2.15	-9.01	-11.28	2.27
MN296	736.75	-.15	79.36	-2.47	-9.20	-11.47	2.26
MN297	736.85	-1.18	78.04	-2.79	-9.76	-11.66	1.90
MN298	736.91	-2.68	76.56	-3.20	-10.96	-11.91	.96
MN299	736.95	-4.29	75.60	-3.51	-12.23	-12.12	-.12
MN300	736.99	-5.94	74.89	-3.76	-13.64	-12.27	-1.37
MN301	737.03	-6.79	74.04	-4.08	-14.21	-12.46	-1.74

STATION	THEORETICAL GRAVITY (MGAL) 979000+	FREE-AIR ANOMALY (MGAL)	REGIONAL ELEVATION (METRES)	REGIONAL FREE-AIR ANOMALY (MGAL)	BOUGUER ANOMALIES AT 2.67 (MGAL)		
					RAW	REGIONAL	RESIDUAL
MN302	737.13	-7.22	73.37	-4.36	-14.45	-12.62	-1.82
MN303	737.20	-7.47	71.54	-4.97	-14.52	-12.96	-1.56
MN304	737.26	-7.22	70.37	-5.30	-14.60	-13.13	-1.47
MN305	737.33	-7.22	69.11	-5.63	-14.69	-13.30	-1.39
MN306	737.40	-7.34	67.72	-5.97	-14.86	-13.49	-1.37
MN307	737.47	-7.25	66.29	-6.22	-15.02	-13.53	-1.49
MN308	737.63	-7.13	62.28	-6.76	-15.19	-13.48	-1.71
MN309	737.70	-7.22	60.22	-6.99	-15.15	-13.46	-1.68
MN310	737.77	-6.98	58.21	-7.21	-15.14	-13.45	-1.69
MN312	738.09	-8.24	50.20	-8.10	-14.29	-13.37	-.92
MN313	738.28	-8.55	47.27	-8.42	-14.20	-13.35	-.85
MN314	738.44	-8.60	44.02	-8.78	-13.85	-13.32	-.53
MN315	738.47	-8.94	43.01	-8.89	-13.72	-13.31	-.41

APPENDIX E : Base Stations

In order to allow future surveys to tie-in to this survey, details of the base stations are furnished here.

Base runs were all tied by a minimum of four individual circuits, each tie being completed in less than 30 minutes. Ties were made to the Australian Isogal Network through Adelaide's main Isogal Station (6091.0108) at Kensington Gardens.

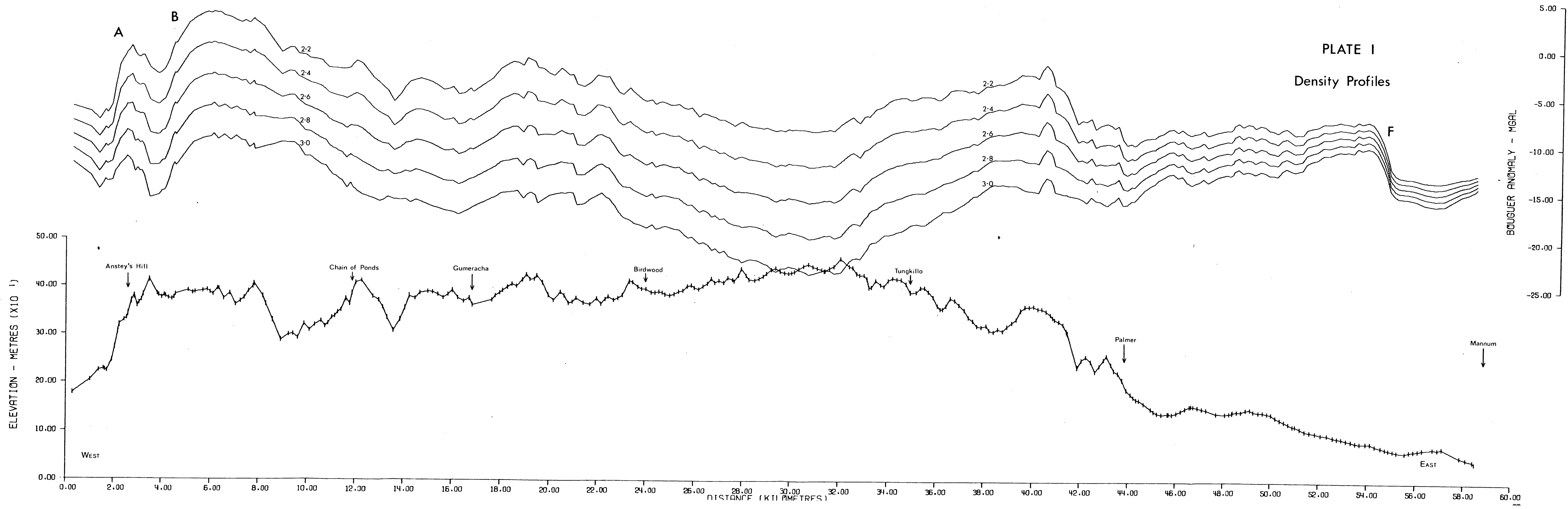| Station Number	Identification	Absolute Gravity Adopted (mgal)	Remarks
AO 011	Anstey's Hill, E & WS Bench Mark 64A	979 659.20	Corner of old stone ruin
GO 073	Approaching Gumeracha, prior to crossing River Torrens. Near E & WS B.M.50.	658.22	Eastern side of main road; south-western corner of first cement support
BO 123	Birdwood. E & WS B.M.38	640.80	On west side of road 100 m from pipe; beside fence post at inflexion of road bend
TO 177	Approaching Tungkillo; crossing main road to Mt. Pleasant	635.77	By cement support of gate, west side of main road.
PO 251	Just east of Palmer. E & WS B.M.16.	694.85	By eastern corner fence-post where dirt road goes south of main road.
Mannum (MN 314)	Playground by River; next to memorial of an old steam boiler	725.14	Reading made at ground level on eastern side of memorial, beside plaque inscribed "First boiler to supply steam for navigation..."

Station numbering gives the key to the main base station used in obtaining an observed gravity. For example, a station prefixed by the letters AH was measured relative to the base station at Anstey's Hill.

Abbreviations used are as follows:-

AH	–	Anstey's Hill
GA		Gumeracha
BW		Birdwood
TK		Tungkillo
PM		Palmer
MN		Mannum

If a station on the traverse is actually a base station, the second letter of the prefix is deleted and a zero inserted, e.g. AO 011 is the Anstey's Hill base station.

Detailed plans of the stations are lodged with the Department of Economic Geology, University of Adelaide.
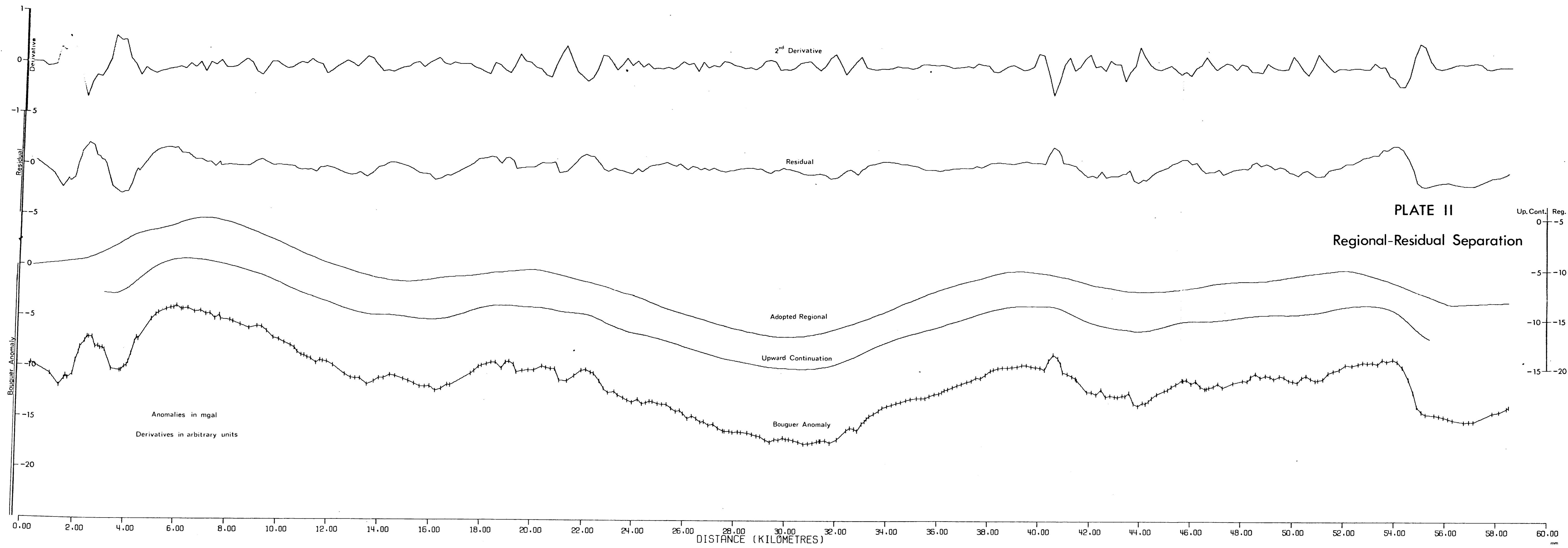
PLATE I

Density Profiles

PLATE II

Regional-Residual Separation

2nd Derivative

Residual

Adopted Regional

Upward Continuation

Bouguer Anomaly

Anomalies in mgal

Derivatives in arbitrary units

DISTANCE (KILOMETRES)

PLATE III
Residual Density Profiles